AD-A177 557 BUCKLING OF DELAMINATED LONG PANELS UNDER PRESSURE AND OF RADIALLY-LOADED (U) GEORGIA INST OF TECH ATLANTA SCHOOL OF ENGINEERING SCIENCE AN... G J SIMITSES ET AL. 1/1

UNCLASSIFIED OCT 85 AFOSR-TR-86-2076 AFOSR-86-0038 F/G 20/11 NL

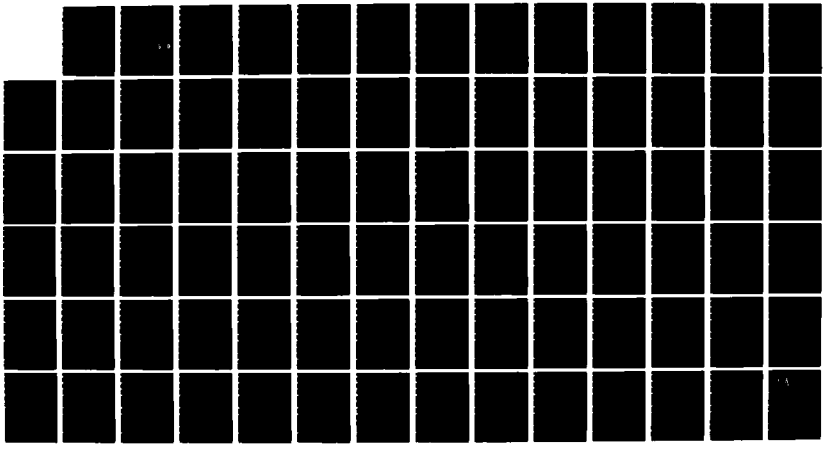

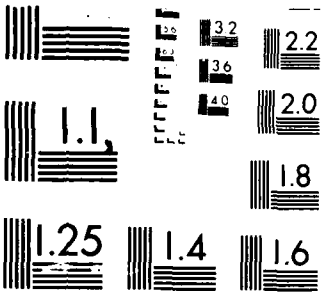

SECURITY CLASSIFICATION OF THIS PAGE (When Data Entered)

REPORT DOCUMENTATION PAGE

READ INSTRUCTIONS BEFORE COMPLETING FORM

1. REPORT NUMBER: AFOSR TR- 86-2076	2. GOVT ACCESSION NO.
3. RECIPIENT'S CATALOG NUMBER	
4. TITLE (and Subtitle): BUCKLING OF DELAMINATED LONG PANELS UNDER PRESSURE AND OF RADIALLY-LOADED STIFFENED ANNULAR PLATES	5. TYPE OF REPORT & PERIOD COVERED: FINAL Dec. 15, 1985 - Sept.15, 198
	6. PERFORMING ORG. REPORT NUMBER
7. AUTHOR(s): George J. Simitses, Y. Frostig and Z. Chen	8. CONTRACT OR GRANT NUMBER(s): AFOSR 86-0038
9. PERFORMING ORGANIZATION NAME AND ADDRESS: Georgia Institute of Technology, School of Engineering Science and Mechanics, 225 North Avenue, S.W., Atlanta, GA 30332	10. PROGRAM ELEMENT, PROJECT, TASK AREA & WORK UNIT NUMBERS: 612300, 2307/B1, 61102F
11. CONTROLLING OFFICE NAME AND ADDRESS: AFOSR/NA, Building 410, Bolling AFB, D.C. 20332	12. REPORT DATE: October 1985
	13. NUMBER OF PAGES: 78
14. MONITORING AGENCY NAME & ADDRESS(if different from Controlling Office): SAME AS 11	15. SECURITY CLASS. (of this report): Unclassified
	15a. DECLASSIFICATION/DOWNGRADING SCHEDULE

16. DISTRIBUTION STATEMENT (of this Report)

Approved for public release; distribution unlimited

17. DISTRIBUTION STATEMENT (of the abstract entered in Block 20, if different from Report)

DTIC ELECTE MAR 0 6 1987 S D

18. SUPPLEMENTARY NOTES

19. KEY WORDS (Continue on reverse side if necessary and identify by block number)

Laminated shells; Delamination Buckling; Damage Tolerance; Annular Plates; Plates with Holes; Laminated Circular Plates.

20. ABSTRACT (Continue on reverse side if necessary and identify by block number)

The buckling of delaminated, long, thin, cylindrical shells and panels is investigated. The thin panels are pressure-loaded and their geometry is quasi-isotropic. The effects of boundary conditions, delamination size, and delamination position on the buckling load are studied. Moreover, the buckling analysis of multi-annular, laminated plates is presented. The annular sections are made of different materials, their size is varied, and the composite circular plates are supported in various ways. Stiffened plates, full or annular, are also analyzed.

DD FORM 1 JAN 73 1473 EDITION OF 1 NOV 65 IS OBSOLETE

SECURITY CLASSIFICATION OF THIS PAGE (When Data Entered)

AD-A177 557

FILE COPY

87 2 25 132

DISCLAIMER NOTICE

THIS DOCUMENT IS BEST QUALITY PRACTICABLE. THE COPY FURNISHED TO DTIC CONTAINED A SIGNIFICANT NUMBER OF PAGES WHICH DO NOT REPRODUCE LEGIBLY.

BUCKLING OF DELAMINATED LONG PANELS UNDER PRESSURE AND OF RADIALLY-LOADED STIFFENED ANNULAR PLATES

by

George J. Simitses[+], Yeoshua Frostig[++]
and Ziqi Chen[+++]
School of Engineering Science and Mechanics
Georgia Institute of Technology, Atlanta, GA.

* This work was supported by the United States Air Force Office of Scientific Research under Grant AFOSR-86-0038.

+ Professor and Principal Investigator

++ Postdoctoral Fellow

+++ Graduate Research Assistant

SUMMARY

The report summarizes the work of the last year under the general heading "Effect of Local Material Imperfections on the Buckling Behavior of Composite Structural Elements". The report contains two parts. The first part deals with delamination buckling of pressure-loaded long cylindrical shells and panels, and the second with buckling of radially-loaded annular plates of laminated construction with or without radial stiffeners.

In part A, the geometry is virtually isotropic and the emphasis is on assessing the effect of delamination position and size on the critical pressure. The boundary conditions on the panels are either simply supported or clamped at circumferential positions. Note that the cylindrical shells or panels are extremely long and the delamination extends along the entire length.

In part B the circular annular plates are subjected to uniform radial compression around the circumference. Laminated and isotropic geometries are used. For the isotropic geometries the effect of plate and stiffener rigidities on the buckling load are fully assessed. Moreover, the effect of boundary conditions is also studied. Finally, for the laminated geometry, a solution procedure is presented, and demonstrated through a laminated geometry that yields a primary state which has a uniform state of stress (symmetric and quasi-isotropic in extension).

CONTENTS

		Page
SUMMARY		ii
PART A:	BUCKLING OF DELAMINATED, LONG CYLINDRICAL PANELS UNDER PRESSURE	1
	1. Introduction	1
	2. Mathematical Formulation	1
	2.1 Description of the Delamination Problem	5
	3. Solution Procedure	13
	4. Numerical Results	23
	5. References	27
	6. Figures and Tables	30
PART B:	BUCKLING AND ANNULAR PLATES	38
I.	EFFECT OF BOUNDARY CONDITIONS AND RIGIDITIES ON THE BUCKLING OF ANNULAR PLATES	39
	1. Introduction	39
	2. Mathematical Formulation	40
	3. Numerical Examples	43
	3.1 Primary State Distributions	44
	3.2 Simply Supported Multi-Annular Plates	47
	3.3 Clamped Multiannular Plates	57
	3.4 Analysis of a Ring-Stiffened Plate Using Plate Theory	61
	4. Conclusions	64
	5. References	65
II.	BUCKLING OF LAMINATED CIRCULAR PLATES	67
	1. Introduction	67
	2. Mathematical Formulation	67
	3. Solution of Buckling Equations	69
	4. Numerical Results	71
	5. References	72
	6. Appendices A and B	72

BUCKLING OF DELAMINATED, LONG, CYLINDRICAL PANELS UNDER PRESSURE.

George J. Simitses[+] and Ziqi Chen[++]
School of Engineering Science and Mechanics
Georgia Institute of Technology, Atlanta, Georgia

Abstract

Delamination is one of the basic defects inherent to laminar materials. The investigation of the buckling characteristics of delaminated cylindrical shells or panels, when subjected to external pressure, is presented herein. The geometry is such that it covers a wide range of length to radius ratios as well as panels of different widths. Results are presented only for very long cylinders and panels. The boundaries are either simply supported or clamped. Furthermore, the material is such that it leads to (quasi) isotropic laminates for all sections involved; the overall as well as the ones separated by the delamination. Finally, the geometry is free of initial geometric imperfections. Because of the last two assumptions, a primary membrane state exists and bifurcational buckling is possible. Buckling load are calculated for a wide range of parameters. The width and the through-the-thickness position of delamination greatly affect the bifurcation load.

1. Introduction

Cylindrical shells and panels are widely used as primary structures in several applications. These are often subjected to destabilizing loads. Therefore, buckling is an important failure mode and it forms a fundamental consideration in the design of such systems.

The advent of fiber reinforced composite materials has resulted in a significant increase of their use as a construction material, because of their many advantages, especially their high potential weight and overall

---

[+]Professor
[++]Graduate Research Assistant

costs savings. It was deemed necessary then to investigate the buckling characteristics of laminated cylindrical shells. Initially, the studies were confined to configurations, which are free of defects, such as delaminations.

In 1975, Tennyson [1] presented a review of all previous studies on the problem. Most of these studies employed the classical approach and dealt with individual and combined application of uniform axial compression, pressure and torsion. Hirano [2] investigated the buckling of angle-ply laminated circular cylinders and obtained the best lamination angles which give the highest buckling stress. There are also some papers about the stability of triple-layered anisotropic cylindrical shells [3-5] and sandwich panels [6].

The stability of geometrically imperfect, laminated cylindrical shells were investigated by Simitses, Shaw and Sheinman [7-10]. The governing equations for the nonlinear analysis of imperfect, stiffened, laminated, circular, cylindrical thin shells, subjected to uniform axial compression and torsion, and supported in various ways, were derived and presented. Two types of formulations were developed, one (W, F formulations) based on Donnell-type nonlinear kinematic relations and the other (U, V, W Formulation) based on Sanders-type.

The buckling of laminated cylindrical panels was studied in recent years also. Zhang and Matthews [11,12] considered panels under four kinds of boundary conditions subjected to the combination of axial compression and shear forces. Two coupled, fourth-order partial differential equations were solved by the use of multiple Fourier series. Numerical computations were performed for a number of panels with different lay-ups, different curvatures and different materials.

Whitney [13] studied the buckling of anisotropic cylindrical panels under arbitrary combinations of axial load, internal pressure and in-plane shear load. He used Donnell-type equations in conjunction with Galerkin's method to determine critical loads.

Buckling and initial postbuckling behavior of symmetrically laminated, thin cross-ply cylindrical panels under axial compression was investigated by Hui [14]. He obtained closed form solutions for the buckling loads. The initial asymmetric postbuckling behavior was demonstrated by computing the postbuckling coefficients.

Composite structures often contain delaminations. Causes of delamination are many and include tool drops, bird strikes, runway debris hits, and manufacturing defects. The presence of delamination in a composite material may cause local buckling and therefore a reduction in the overall load bearing capacity of the structure. The problem of delamination buckling has received attention in recent years.

A finite element analysis was developed by Whitcomb [15] to analyze a laminated plate with a through-the-width delamination. The postbuckling behavior was studied. In the parametric study, stress distributions and strain-energy release rates were calculated for various delamination lengths, delamination depths, applied loads, and lateral deflections. Some delamination growth data were obtained through fatigue tests. Another paper in this subject was presented by the above author and Shivakumar [26], in 1985, in which the buckling of an elliptic delamination embedded near the surface of a thick quasi-isotropic laminate was studied. Both the Finite Element and the Rayleigh-Ritz methods were used for the analysis. The Rayleigh-Ritz method was found to be simple, inexpensive, and accurate, except for highly anisotropic delaminated regions. In that paper, effects

of delamination shape and orientation, material anisotropy, and layup on buckling strains were examined.

Yin and Wang [17] derived a simple expression for the energy release rate associated with the growth of a general one-dimensional delamination. The energy release rate was evaluated by means of the path-independent J-integral. Yin and Fei [28] investigated the buckling load of a circular plate with a concentric delamination.

Angle-ply composite sandwich beams with through-the-width delaminations were studied by Gillespie and Pipes [19]. Reduction in flexural strength was found to be directly proportional to the length of delamination and varied from 41% to 87% of the pristine value.

S. S. Wang [20] investigated the buckling of angle-ply composite laminates with edge delamination. Based on a recently developed theory of laminated anisotropic elasticity, the problem was formulated using Lekhnitskii's complex variable stress potentials. An eigenfunction expansion method was employed to solve the singular elasticity problem. With the aid of a boundary collocation technique, complete stress and displacement fields were obtained.

A two-dimensional analytical model was developed by Chai and Babcock [21] to assess the compressive strength of near-surface interlaminar defects in laminated composites. The postbucking solution for the delaminated elliptic sections was obtained by using the Rayleigh-Ritz method, while an energy balance criterion based on a self-similar disbond growth governed fracture.

Simitses, Sallam and Yin [22-24] investigated the delamination buckling and growth of flat composite structural elements. A simple one-dimensional model was developed to predict critical loads for

delaminated plates with both simply supported and clamped ends. The effects of delamination positon, size, and thickness on the critical loads were studied in detail. The postbuckling behavior as well as the energy release rate were examined. The results revealed that the damage tolerance of the laminate was either governed by buckling or by the fracture toughness of the material.

Almost all the papers about delamination buckling deal with beams and plates. Owing to its complexity in mathematics, very limited information on the subject of delamination buckling of shells is currently available.

Troshin [25] studied the effect of longitudinal delamination, in a laminar cylindrical shell, on the critical external pressure. The shell was assumed to be separated by the delamination into three panels. A system of eight ordinary differential equations were derived from the governing partial differential equations. The system along with boundary and continuity conditions was integrated by the Kutta-Merson method with intermediate orthonormalization of solution vectors. Critical pressures for various locations and sizes of the delamination were found. In another paper [26], the above author investigated the delamination stability of triple-layered shells with almost the same method. Sallam and Simitses [27] studied delaminations buckling of thin cylindrical shells of perfect geometry, when subjected to uniform axial compression. The delamination region was assumed to be of constant width and covering the entire circumference.

2. Mathematical Formulation

The Koiter-Budiansky [28] buckling equations have been deduced from those given in the Appendix of [28]. They are given below in terms of

stress, N_{jj}, and moment, M_{jj}, resultants for a thin, circular, cylindrical shell under uniform pressure.

$$
\begin{aligned}
&N_{xx,x} + N_{xy,y} - \frac{1}{2R} M^{*}_{xy,y} + qR \left(\frac{1}{2}\gamma^{o}_{xy} - \phi_z\right)^{*}_{,y} + q^x = 0 \\
&N_{xy,x} + N_{yy,y} + \frac{1}{R}\left(M_{yy,y} + M_{xy,x}\right)^{**} + \frac{1}{2R} M^{*}_{xy,x} \\
&\qquad + q\,R\left(\varepsilon^{o^{*}}_{yy,y} - \frac{\phi_y^{**}}{R}\right) + q^y = 0 \\
&-N_{yy}/R + M_{xx,xx} + 2M_{xy,xy} + M_{yy,yy} - qR\left(\phi_{y,y} + \frac{\varepsilon^{o^{*}}_{yy}}{R}\right) \\
&\qquad + q\left(\varepsilon^{o}_{xx} + \varepsilon^{o}_{yy}\right)^{*} + q^z = 0
\end{aligned}
\tag{1}
$$

where ϕ_x, ϕ_y and ϕ_z are rotations about axes denoted by the subscripts, q^x, q^y and q^z are corrections to surface loading due to load behavior during buckling, q is the applied pressure ε^{o}_{xx}, ε^{o}_{yy} and γ^{o}_{xy} are the reference surface small additional strains (needed to take us from the primary membrane state to the infinitesimally close buckled state), and R is the radius of the reference cylindrical surface. Note also that if the terms denoted by a single asterisk are dropped the equations, Eqs. (1), correspond to those obtained from Sanders type of kinematic relations [29]. Similarly, if terms marked by either single or double asterisk are dropped one obtains the well known Donnell-type of equations.

Since there exist three possibilities of load behavior during the buckling process [30,31], the corrections to surface loading assume three distinctly different expressions.

I. Load remains normal to the deformed surface

$$q^x = -qw_{,x} \; ; \; q^y = -q\left(w_{,y} - \frac{v^{**}}{R}\right) \; ; \; q^z = 0 \tag{2a}$$

II. Load remains constant-directional

$$q^x = q^y = q^z = 0 \tag{2b}$$

III. Load remains directed towards initial center of curvature

$$q^x = 0 \; ; \; q^y = q\frac{v^{**}}{R} \; ; \; q^z = 0 \tag{2c}$$

The kinematic relations are given by

$$\begin{aligned} \epsilon_{xx} &= \epsilon^o_{xx} + zK_{xx} \\ \epsilon_{yy} &= \epsilon^o_{yy} + zK_{yy} \\ \gamma_{xy} &= \gamma^o_{xy} + 2zK_{xy} \end{aligned} \tag{3}$$

where the expressions for the reference surface strains, rotations, ϕ_j, and changes in curvature and torsion, k_{jj}, are given by

$$\epsilon^o_{xx} = u_{,x} \qquad \phi_x = -w_{,x}$$

$$\epsilon^o_{yy} = v_{,y} + \frac{w}{R} \qquad \phi_y = \frac{v^{**}}{R} - w_{,y}$$

$$\gamma^o_{xy} = u_{,y} + v_{,x} \qquad \phi_z = \frac{1}{2}(v_{,x} - u_{,y}) \tag{4}$$

$$K_{xx} = -w_{,xx}$$

$$K_{yy} = -\left(w_{,yy} - \frac{1}{R}v^{**}_{,y}\right)$$

$$K_{xy} = -\left[w_{,xy} - \frac{v^{**}_{,x}}{2R} + \left(\frac{u_{,y}}{4R} - \frac{v_{,x}}{4R}\right)^*\right]$$

The usual lamination theory [32] is employed. Moreover, it is assumed that all shell (laminates) parts are symmetric with respect to their midsurfaces ($B_{jj} \equiv 0$). Then, the stress and moment resultants are related to the reference surface strain parameters by

$$\begin{bmatrix} N_{xx} \\ N_{yy} \\ N_{xy} \end{bmatrix} = \begin{bmatrix} A_{11} & A_{12} & A_{13} \\ A_{12} & A_{22} & A_{23} \\ A_{13} & A_{23} & A_{33} \end{bmatrix} \begin{bmatrix} \epsilon^{o}_{xx} \\ \epsilon^{o}_{yy} \\ \gamma^{o}_{xy} \end{bmatrix}$$

$$\begin{bmatrix} M_{xx} \\ M_{yy} \\ M_{xy} \end{bmatrix} = \begin{bmatrix} D_{11} & D_{12} & D_{13} \\ D_{12} & D_{22} & D_{23} \\ D_{13} & D_{23} & D_{33} \end{bmatrix} \begin{bmatrix} K_{xx} \\ K_{yy} \\ 2K_{xy} \end{bmatrix} \qquad (5)$$

where

$$A_{jj} = \sum_{k=1}^{N} \bar{Q}^{(k)}_{jj} (h_k - h_{k-1})$$

$$D_{jj} = \frac{1}{3} \sum_{k=1}^{N} \bar{Q}^{(k)}_{jj} (h_k^3 - h_{k-1}^3) \qquad (6)$$

and h_k and h_{k-1} denote the z-coordinate of the upper and lower surfaces of the kth lamina in each laminate, respectively.

In terms of the displacement components, u,v and w the buckling equations, Eqs. (1), become

$$A_{11}u_{,xx} + 2A_{13}u_{,xy} + A_{33}\,u_{,yy} + (A_{12} + A_{33})\,v_{,xy} + A_{13}v_{,xx}$$

$$+ A_{23}v_{,yy} + A_{12}\frac{w_{,x}}{R} + \frac{A_{23}}{R}\,w_{,y} + q^x = 0$$

$$A_{13}u_{,xx} + (A_{33} + A_{12})\,u_{,xy} + A_{23}u_{,yy} + (A_{33} + \frac{D_{33}}{R^2})\,v_{,xx}$$

$$+ (2A_{23} + \frac{2D_{23}}{R^2})\,v_{,xy} + (A_{22} + \frac{D_{22}}{R^2})\,v_{,yy} - \frac{qv}{R} + \frac{A_{23}}{R}\,w_{,x}$$

$$+ (\frac{A_{22}}{R} + q)\,w_{,y} - \frac{1}{R}[D_{13}w_{,xxx} + (D_{12} + 2D_{33})\,w_{,xxy} + 3D_{23}w_{,xyy} + \qquad (7)$$

$$D_{22}w_{,yyy}] + q^y = 0.$$

$$-\frac{A_{12}}{R}\,u_{,x} - \frac{A_{23}}{R}\,u_{,y} - \frac{A_{23}}{R}\,v_{,x} - \frac{1}{R}\,(A_{22} + qR)\,v_{,y}$$

$$+ [\frac{D_{13}}{R}\,v_{,xxx} + (\frac{D_{12}}{R} + \frac{2D_{33}}{R})\,v_{,xxy} + \frac{3D_{23}}{R}\,v_{,xyy} + \frac{D_{22}}{R}\,v_{,yyy}] - \frac{A_{22}}{R^2}\,w -$$

$$- [D_{11}w_{,xxxx} + 4D_{13}w_{,xxxy} + (2D_{12} + 4D_{33})\,w_{,xxyy} + 4D_{23}w_{,xyyy} +$$

$$D_{22}w_{,yyyy}] + qRw_{,yy} + q^z = 0$$

Note that these equations correspond to the Sanders' approximation [30] and therefore all asterisks have been dropped.

2.1 Description of the Delamination Problem

Thin circular cylindrical shells and panels with longitudinal delamination over the entire length are next considered. The geometry, loading and coordinate systems are shown on Fig. 1. The ends of the panel are either clamped or simply supported. The location and size of the

delamination is arbitrary. Angle α denotes the region of the delamination, while β and γ denote the location of it from left end and right end, respectively.

It is assumed that under subcritical loads the delamination does not expand. The panel is separated into four parts (four panels) by the delamination. Each part has a set of coordinates attached to it, (see Fig. 1.) and the natural plane of the panel lies on the XY-plane. The panel is subjected to uniform external pressure, q, over the entire outer surface. Let h^i (i = I, II, III, IV) denote the thickness of the ith panel (see Fig. 1). The nondimensional parameter $\bar{h} = h^I/h^{III}$ is used to describe the thickness of the delamination. Let u^i, v^i, w^i (i = I, II, III, IV) be the displacement components of material points on the midplane of each part (each panel) in the x, y, and z directions, respectively.

The panel becomes a complete cylindrical shell when the total angle γ ($\gamma = \alpha + \beta + \gamma$) equals 2π. The geometry is such that a membrane primary state exists ($B^i_{jj} \equiv 0$) for all participating parts. Therefore, the buckling equations, Eqs. (1), apply to each part. They are subject to boundary conditions at $\theta_3 = 0$ and $\theta_4 = \gamma$ (see Fig. 1), and certain kinematic continuity conditions as well as force and moment local equilibrium conditions at the common boundaries of the various parts ($\theta_3 = \beta$ and $\theta_4 = 0$).

Note that all of these conditions are associated with y = constant positions. Each part must also satisfy boundary conditions associated with x = constant positions. These are not listed now, but they correspond to the classical simply supported ones. They are listed in the next section.

The various boundary and auxiliary conditions associated with y = constant positions, are listed below:

Boundary conditions at $\theta_3 = 0$

(a) Clamped

$$w^{III} = 0$$

$$\phi_y^{III} = 0 \qquad (a)$$

$$v^{III} = 0$$

$$u^{III} = 0$$

(b) Simply Supported

$$w^{III} = 0$$

$$M_{yy}^{III} = 0 \qquad (b) \qquad (8)$$

$$N_{yy}^{III} = 0$$

$$u^{III} = 0$$

Auxiliary Condition at $\theta_3 = \beta$ ($\theta_1 = \theta_2 = 0$)

$$w^I = w^{II} = w^{III}$$

$$\phi_y^I = \phi_y^{II} = \phi_y^{III}$$

$$v^I - (v^{III} + \phi_y^{III} h^{II}/2) = 0$$

$$V^{II} - (v^{III} - \phi_y^{III} h^I/2) = 0$$

$$u^I - (u^{III} + \phi_x^{III} h^{II}/2) = 0$$

$$u^{II} - (u^{III} - \phi_x^{III} h^I/2) = 0 \qquad (9)$$

$$N_{yy}^I + N_{yy}^{II} - N_{yy}^{III} = 0$$

$$N_{xy}^I + N_{xy}^{II} - N_{xy}^{III} = 0$$

$$M_{yy}^I + N_{yy}^I h^{II}/2 + M_{yy}^{II} - N_{yy}^{II} h^I/2 - M_{yy}^{III} = 0$$

$$Q_{y(eff)}^I + N_{xy,x}^I h^{II}/2 + Q_{y\ (eff)}^{II} - N_{xy,x}^{II} h^I/2 - Q_{y(eff)}^{III} = 0$$

where

$$Q_{y(eff)} = M_{yy,y} + 2M_{xy,x}$$

Auxiliary Conditons at $\theta_4 = 0$ ($\theta_1 = \theta_2 = \alpha$)

$$w^I = w^{II} = w^{III}$$

$$\phi_y^I = \phi_y^{II} = \phi_y^{III}$$

$$v^{II} - (v^{IV} + \phi_y^{IV} h^{II}/2) = 0$$

$$v^{II} - (v^{IV} - \phi_y^{IV} h^I/2) = 0$$

$$u^I - (u^{IV} + \phi_x^{IV} h^{II}/2) = 0 \qquad (10)$$

$$u^{II} - (u^{IV} - \phi_x^{IV} h^I/2) = 0$$

$$N_{yy}^I + N_{yy}^{II} - N_{yy}^{IV} = 0$$

$$N_{xy}^I + N_{xy}^{II} - N_{xy}^{IV} = 0$$

$$M_{yy}^I + N_{yy}^I h^{II}/2 + M_{yy}^{II} - N_{yy}^{II} h^I/2 - M_{yy}^{IV} = 0$$

$$Q_{y(eff)}^I + N_{xy,x}^I h^{II}/2 + Q_{y(eff)}^{II} - N_{xy,x}^{II} h^I/2 - Q_{y(eff)}^{IV} = 0$$

Boundary Conditions at $\theta_4 = \gamma$

(a) Clamped		(b) Simply Supported		
$w^{IV} = 0$		$w^{IV} = 0$		
$\phi_y^{IV} = 0$	(a)	$M_{yy}^{IV} = 0$	(b)	(11)
$v^{IV} = 0$		$N_{yy}^{IV} = 0$		
$u^{IV} = 0$		$u^{IV} = 0$		

Note that the simply supported conditions, Eqs. (8b) and (11b) correspond to the classical simply supported conditions, SS-3 [32].

3. Solution Procedure

For each part, a separated solution is assumed, which satisfies the classical simply supported boundary condtions at x = 0 and L. This is done for the special construction for which there is no coupling between extension and shear, and between bending and twisting action. This means that for all parts

$$A_{13} = A_{23} = D_{13} = D_{23} = 0 \tag{12}$$

The classical simply supported boundary conditons are denoted by

$$\text{SS3:} \quad w = M_{xx} = N_{xx} = v = 0 \tag{13}$$

The separated solution is characterized by

$$u(x,y) = U(y) \cos \frac{m\pi x}{L}$$

$$u(x,y) = V(y) \sin \frac{m\pi x}{L} \tag{14}$$

$$w(x,y) = W(y) \sin \frac{m\pi x}{L}$$

Substitution of Eqs. (14) into Eqs. (7), for the special construction, Eqs. (12), yields

$$\begin{aligned} L_{11}U + L_{12}V + L_{13}W &= 0 \\ L_{21}U + L_{22}V + L_{23}W &= 0 \\ L_{31}U + L_{32}V + L_{33}W &= 0 \end{aligned} \tag{15}$$

where the L_{jj} are linear differential operators. Their expression is given by

$$L_{11} = -A_{11}(\ ) + \bar{L}^2 A_{33}(\ )''$$

$$L_{12} = (A_{12} + A_{33}) \bar{L}(\ )'$$

$$L_{13} = (A_{12} - \begin{pmatrix} 1 \\ 0 \\ 0 \end{pmatrix} \frac{\lambda D_{11}}{R^2}) \bar{L}$$

$$L_{21} = -(A_{12} + A_{33}) \bar{L} ( )'$$

$$L_{22} = -(A_{33} + \frac{D_{33}}{R^2} + \begin{pmatrix} 0 \\ 1 \\ 0 \end{pmatrix} \frac{\lambda D_{11}}{R^2} \bar{L}^2) ( ) + \bar{L}^2 (A_{22} + \frac{D_{22}}{R^2}) ( )'' \qquad (16)$$

$$L_{23} = (A_{22} + \begin{pmatrix} 0 \\ 1 \\ 1 \end{pmatrix} \frac{\lambda D_{11}}{R^2} \bar{L}^2 ( )' + \frac{1}{R^2} (D_{12} + 2D_{33}) ( )' - \frac{D_{22}}{R^2} \bar{L}^2 ( )'''$$

$$L_{31} = -A_{12} \bar{L} ( )$$

$$L_{32} = A_{22} \bar{L}^2 ( )' + \frac{1}{R^2} (D_{12} + 2D_{33}) ( )' - \frac{D_{22}}{R^2} \bar{L}^2 ( )''' + L^2 \frac{\lambda D_{11}}{R^2} ( )'$$

$$L_{33} = A_{22} \bar{L}^2 ( ) + \frac{D_{11}}{R^2} \frac{1}{\bar{L}^2} ( ) - \frac{2(D_{12} + 2D_{33})}{R^2} ( )''$$

$$+ \frac{D_{22}}{R^2} \bar{L}^2 ( )'''' - \frac{\lambda D_{11}}{R^2} \bar{L}^2 ( )''$$

where the prime denotes differentiation with respect to θ,

$$\bar{L} = L/m\pi R \quad , \quad \theta = y/R, \quad \text{and } \lambda = qR^3/D_{11},$$

and R is the same for all parts.

Elimination of U and V through the use of the first two of Eqs. (15) and through substitution into the third one yields a single higher order ordinary differential equation in W alone. This higher order equation assumes the form

$$F_8 \frac{d^8 w}{d\theta^8} + F_6 \frac{d^6 w}{d\theta^6} + F_4 \frac{d^4 w}{d\theta^4} + F_2 \frac{d^2 w}{d\theta^2} + F_0 = 0 \qquad (17)$$

where the F's are constants that contain the external load q and structural geometric parameters (A_{ij}, D_{ij},$\bar{h}$, R, etc.). Note that some of the F's change according to the case of load behavior during buckling, Eqs. (2).

The expressions for the F's are given below:

$$F_8 = D_{22}\bar{L}^2(a_{33}-a_{23})/R^2$$

$$F_6 = D_{22}\bar{L}^2(a_{32}-a_{22})/R^2 + \lambda D_{11}\bar{L}^2(a_{23}-a_{33})/R^2 +$$

$$(D_{12} + 2D_{33})\,(a_{23}-2a_{33})/R^2 + A_{22}\bar{L}^2 a_{23}$$

$$F_4 = A_{22}\bar{L}^2\,(a_{33} + a_{22}) + (D_{12} + 2D_{33})(a_{22} - 2a_{32})/R^2 + D_{11}a_{33}/(\bar{L}R)^2 \qquad (18)$$

$$+ \lambda D_{11}\bar{L}^2(a_{22} - a_{32})/R^2 + D_{22}\bar{L}^2(a_{31} - a_{21})/R^2 - A_{12}\bar{L}a_{13}$$

$$F_2 = \lambda D_{11}\bar{L}^2\,(a_{21} - a_{31})/R^2 + (D_{12} + 2D_{33})\,(a_{21} - 2a_{31})/R^2 +$$

$$A_{22}\bar{L}^2\,(a_{21} + a_{32}) + D_{11}a_{32}/(\bar{L}R)^2 - A_{12}\bar{L}a_{12}$$

$$F_0 = A_{22}\bar{L}^2 a_{31} + D_{11}a_{31}/(\bar{L}R)^2 - A_{12}\bar{L}a_{11}$$

where

$$a_{11} = -\left[A_{12} - \begin{pmatrix}1\\0\\0\end{pmatrix}\frac{\lambda D_{11}}{R^2}\right]\left[A_{33} + \frac{D_{33}}{R^2} + \begin{pmatrix}0\\1\\0\end{pmatrix}\frac{\lambda D_{11}\bar{L}^2}{R^2}\right]\bar{L}$$

$$a_{12} = \bar{L}^3 \left(A_{12} - \begin{pmatrix} 1 \\ 0 \\ 0 \end{pmatrix} \frac{\lambda D_{11}}{R^2}\right)\left(A_{22} + \frac{D_{22}}{R^2}\right) - (A_{12} + A_{33})\left[\bar{L}^3\left(A_{22} + \begin{pmatrix} 0 \\ 1 \\ 1 \end{pmatrix} \frac{\lambda D_{11}}{R^2}\right) + \bar{L}\,(D_{12} + 2D_{33})/R^2\right]$$

$$a_{13} = (A_{12} + A_{33})\, D_{22}\bar{L}^3/R^2$$

$$a_{21} = -A_{11}\left[\left(A_{22} + \begin{pmatrix} 0 \\ 1 \\ 1 \end{pmatrix} \frac{\lambda D_{11}}{R^2}\right)\bar{L}^2 + (D_{12} + 2D_{33})/R^2\right] + \left(A_{12} - \begin{pmatrix} 1 \\ 0 \\ 0 \end{pmatrix} \frac{\lambda D_{11}}{R^2}\right)(A_{12} + A_{33})\,\bar{L}^2$$

$$a_{22} = A_{33}\left[\left(A_{22} + \begin{pmatrix} 0 \\ 1 \\ 1 \end{pmatrix} \frac{\lambda D_{11}}{R^2}\right)\bar{L}^4 + \frac{\bar{L}^2}{R^2}(D_{12} + 2D_{33})\right] + \frac{A_{11}D_{22}\bar{L}^2}{R^2} \qquad (19)$$

$$a_{23} = -A_{33}D_{22}\bar{L}^4/R^2$$

$$a_{31} = -A_{11}\left(A_{33} + \frac{D_{33}}{R^2} + \begin{pmatrix} 0 \\ 1 \\ 0 \end{pmatrix} \frac{\lambda D_{11}\bar{L}^2}{R^2}\right)$$

$$a_{32} = A_{11}\left(A_{22} + \frac{D_{22}}{R^2}\right)\bar{L}^2 + \left(A_{33} + \frac{D_{33}}{R^2} + \begin{pmatrix} 0 \\ 1 \\ 0 \end{pmatrix} \frac{\lambda D_{11}\bar{L}^2}{R^2}\right) A_{33}\bar{L}^2 - (A_{12} + A_{33})^2\,\bar{L}^2$$

$$a_{33} = -\bar{L}^4 A_{33}(A_{22} + D_{22}/R^2)$$

The column vector in the expressions for a_{ij} denote the load cases as described by Eqs. (2).

The solution procedure is similar to the one described for rings and arches in Article 7.3 of Ref. 34. The number of equations is higher, the equations themselves are more complex, and a closed formed solution is not expected as in Ref. 33. Nevertheless, the overall procedure can be followed and a numerical estimate can be achieved.

The basic steps are as follows:

First assume for $W(\theta)$ a solution of the form

$$W = C\, e^{r\theta} \tag{20}$$

Since the order of the equation is eight, then substitution into Eq. (17) yields an eighth degree polynomial in r. Thus, eight roots are expected for each geometry and load level. If the eight roots are distinctly different, the general solution for $W(\theta)$ is given by

$$W(\theta) = \sum_{i=1}^{8} C_i\, e^{r_i\theta} \tag{21}$$

Note that if double roots occur the form of Eq. (21) is modified accordingly.

The form of the solution for $U(\theta)$ and $V(\theta)$ is similar to that of Eq. (21), or

$$U(\theta) = \sum_{j=1}^{8} A_j e^{r_j\theta}$$

$$V(\theta) = \sum_{j=1}^{8} B_j e^{r_j\theta} \tag{22}$$

Note that in deriving Eq. (17), U and V were eliminated through operations on Eqs. (15). The intermediate steps that lead to this elimination yield

$$(L_{21}L_{12} - L_{11}L_{22})\, U = (L_{13}L_{22} - L_{12}L_{23})\, W$$

$$(L_{21}L_{12} - L_{11}L_{22})\, V = (L_{11}L_{23} - L_{13}L_{21})\, W \tag{23}$$

Substitution of Eqs. (21) and (22) into Eqs. (23) yields the expressions of A_i and B_i in terms of C_j, or

$$A_j = \xi_j C_j$$

$$B_j = n_j C_j \qquad \text{for } i = 1,2,\ldots 8 \tag{24}$$

where

$$\xi_j = (a_{11} + r_j^2 a_{12} + r_j^4 a_{13})/(a_{31} + r_j^2 a_{32} + r_j^4 a_{33})$$

$$n_j = (a_{21} r_j + r_j^3 a_{22} + r_j^5 a_{23})/(a_{31} + r_j^2 a_{32} + r_j^4 a_{33}) \tag{24a}$$

Thus, the solution for U, V, and W is given in terms of eight constants C_j, while ξ_j and n_i are known.

$$U(\theta) = \sum_{j=1} \xi_j C_j e^{r_j \theta}$$

$$V(\theta) = \sum_{j=1}^{8} n_j C_j e^{r_j \theta} \tag{25}$$

$$W(\theta) = \sum_{i=1}^{8} C_j e^{r_j \theta}$$

There exist eight unknowns, C_j's, for each panel. Since there exist four panels because of the delamination, the total number of unknowns is 32. Use of the 32 boundary and auxiliary conditions, Eqs. (8)-(11), leads to a system of 32 linear homogeneous algebraic equations in the 32 unknowns. A nontrivial solution exists if the determinant of the coefficients vanishes.

This is the characteristic equation, which yields the value of the critical load. A numerical procedure has been developed to accomplish this.

For the sake of completeness, the boundary and auxiliary conditions are presented in terms of the respective displacement functions, u, v and w [see Eqs. (8)-(11)].

Boundary Conditions at $\theta_3 = 0$

(a) Clamped

$$u^{III} = 0$$

$$v^{III} = 0$$

$$w^{III} = 0 \qquad \text{(a)}$$

$$(v - w_{,\theta})^{III} = 0$$

(b) Simply Supported

$$u^{III} = 0$$

$$A_{12}^{III} Ru_{,x}^{III} + A_{22}^{III} (v_{,\theta} + w)^{III} = 0.$$

$$W^{III} = 0 \qquad \text{(b)} \qquad (26)$$

$$-R^2 D_{12}^{III} w_{,xx}^{III} - D_{22}^{III} (w_{,\theta\theta} - v_{,\theta})^{III} = 0$$

Auxiliary Conditions at $\theta_3 = \beta$

$$w^{I} = w^{II} = w^{III}$$

$$(v - w_{,\theta})^{I} = (v - w_{,\theta})^{II} = (v - w_{,\theta})^{III}$$

$$v^{I} - [v^{III} + \frac{1}{R} (v^{I} - w_{,\theta}^{I}) h^{II}/2] = 0$$

$$v^{II} - [v^{III} - \frac{1}{R} (v^{I} - w_{,\theta}^{I}) h^{I}/2] = 0$$

$$u^{I} - [u^{III} - w_{,x}^{III} h^{II}/2] = 0$$

$$u^{II} - [u^{III} + w_{,x}^{III} h^{I}/2] = 0$$

$$[R A_{12}u_{,x} + A_{22}(v_{,\theta} + w)]^{I} + [RA_{12}u_{,x} + A_{22}(v_{,\theta} + w)]^{II}$$

$$- [R A_{12}u_{,x} + A_{22}(v_{,\theta} + w)]^{III} = 0$$

$$[A_{33}(u_{,\theta} + Rv_{,x})]^{I} + [A_{33}(u_{,\theta} + Rv_{,x})]^{II} - [A_{33}(u_{,\theta} + Rv_{,x})]^{III} = 0$$

$$[-D_{12}w_{,xx} - \frac{D_{22}}{R^2}(w_{,\theta\theta} - v_{,\theta})]^{I} + [A_{12}u_{,x} + A_{22}(v_{,\theta} + w)\frac{1}{R}]^{I}h^{II}/2$$

$$+ [-D_{12}w_{,xx} - \frac{D_{22}}{R^2}(w_{,\theta\theta} - v_{,\theta})]^{II} - [A_{12}u_{,x} + A_{22}(v_{,\theta} + w)\frac{1}{R}]^{II}h^{I}/2$$

$$+ [-D_{12}w_{,xx} + \frac{D_{22}}{R^2}(w_{,\theta\theta} - v_{,\theta})]^{III} = 0$$

$$[-D_{12}\frac{1}{R}w_{,xx\theta} - \frac{1}{R^3}D_{22}(w_{,\theta\theta\theta} - v_{,\theta\theta})]^{I} - 4D_{33}^{I}(\frac{1}{R}w_{,xx\theta} - \frac{1}{2R}v_{,xx})^{I}$$

$$+ [A_{33}(\frac{1}{R}u_{,\theta x} + v_{,xx})]^{I}h^{II}/2$$

$$- [D_{12}\frac{1}{R}w_{,xx\theta} + \frac{1}{R^3}D_{22}(w_{,\theta\theta\theta} - v_{,\theta\theta})]^{II} - 4D_{33}^{II}[\frac{1}{R}w_{,xx\theta} - \frac{1}{2R}v_{,xx}]^{II}$$

$$- [A_{33}(\frac{1}{R}u_{,\theta x} + v_{,xx})]^{II}h^{I}/2$$

$$+ [D_{12}\frac{1}{R}w_{,xx\theta} + \frac{1}{R^3}D_{22}(w_{,\theta\theta\theta} - v_{,\theta\theta})]^{III} + 4D_{33}^{III}[\frac{1}{R}w_{,xx\theta} - \frac{1}{2R}v_{,xx}]^{III} = 0$$

Auxiliary Conditions at $\theta_1 = \theta_2 = \alpha$

$$w^I = w^{II} = w^{III}$$

$$(v - w_{,\theta})^I = (v - w_{,\theta})^{II} = (v - w_{,\theta})^{III}$$

$$v^I - [v^{IV} + \frac{1}{R}(v^{IV} - w_{,\theta}{}^{IV})\ h^{II}/2] = 0$$

$$v^{II} - [v^{IV} - \frac{1}{R}(v^{IV} - w_{,\theta}{}^{IV})\ h^I/2] = 0$$

$$u^I - [u^{IV} - w_{,x}{}^{IV}\ h^{II}/2] = 0$$

$$u^{II} - [u^{IV} + w_{,x}{}^{IV} h^I/2] = 0$$

$$[R\ A_{12}u_{,x} + A_{22}(v_{,\theta} + w)]^I + [RA_{12}u_{,x} + A_{22}(v_{,\theta} + w)]^{II}$$

$$- [R\ A_{12}u_{,x} + A_{22}\ (v_{,\theta} + w)]^{IV} = 0$$

$$[A_{33}(u_{,\theta} + Rv_{,x})]^I + [A_{33}(u_{,\theta} + Rv_{,x})]^{II} - [A_{33}(u_{,\theta} + Rv_{,x})]^{IV} = 0$$

$$[- D_{12}w_{,xx} - \frac{D_{22}}{R^2}(w_{,\theta\theta} - v_{,\theta})]^I + [A_{12}u_{,x} + A_{22}(v_{,\theta} + w)\ \frac{1}{R}\ ]^I\ h^{II}/2$$

$$- [D_{12}w_{,xx} + \frac{D_{22}}{R^2}(w_{,\theta\theta} - v_{,\theta})\ ]^{II} - [A_{12}u_{,x} + A_{22}\ (v_{,\theta} + w)\ \frac{1}{R}\ ]^{II}\ h^I/2$$

$$+ [D_{12}\ w_{,xx} + \frac{D_{22}}{R^2}\ (w_{,\theta\theta} - v_{,\theta})\ ]^{IV} = 0$$

$$[-D_{12}\ \frac{1}{R}\ w_{,xx\theta} - \frac{1}{R^3}\ D_{22}(w_{,\theta\theta\theta} - v_{,\theta\theta})]^I - 4D_{33}^I\ [\ \frac{1}{R}\ w_{,xx\theta} - \frac{1}{2R}\ v_{,xx}]$$

$$+ [A_{33} (\frac{1}{R} u,_{\theta x} + v,_{xx})]^{I} h^{II}/2 + [- D_{12} \frac{1}{R} w,_{xx\theta} - \frac{1}{R^3} D_{22}(w,_{\theta\theta\theta} - v,_{\theta\theta})]^{II}$$

$$-4D_{33}^{II} [\frac{1}{R} w,_{xx\theta} - \frac{1}{2R} v,_{xx}]^{II} - [A_{33} (\frac{1}{R} u,_{\theta x} + v,_{xx})]^{II} h^{I}/2$$

$$+ [D_{12} \frac{1}{R} w,_{xx\theta} + \frac{1}{R^3} D_{22}(w,_{\theta\theta\theta} - v,_{\theta\theta})]^{IV} + 4D_{33}^{IV} [\frac{1}{R} w,_{xx\theta} - \frac{1}{2R} v,_{xx}]^{IV} = 0$$

Boundary Conditions at $\theta_4 = \gamma$

(a) Clamped

$$u^{IV} = 0$$

$$v^{IV} = 0$$

(a)

$$w^{IV} = 0$$

$$(v - w,_{\theta})^{IV} = 0$$

(b) Simply Supported

$$u^{IV} = 0$$

$$A_{12}^{IV} Ru,_{x}^{IV} + A_{22}^{IV} (v,_{\theta} + w)^{IV} = 0$$

(b) (29)

$$w^{IV} = 0$$

$$-R^2 D_{12}^{IV} w,_{xx}^{IV} - D_{22}^{IV} (w,_{\theta\theta} - v,_{\theta})^{IV} = 0$$

All of the above conditions can easily be expressed in terms of $U(\theta)$, $V(\theta)$, and $W(\theta)$ instead of u, v, and w. This is so because in all boundary and auxiliary conditions, Eqs. (26)-(29), if the order of differentiation with respect to x, of v and w is even, the one for u is odd, or vice versa [see Eq. (14)]. Thus, in each one of the conditions either $\sin \frac{m\pi x}{L}$ or $\cos \frac{m\pi x}{L}$ is the common factor, which does not vanish for all x.

A computer program has been written in order to obtain critical conditions for all geometries. The Georgia Tech high speed digital computer, CDC Cyber 70, Model 74-28, was used for generation of results.

4. Numerical Results

Results are presented herein only for a special geometry and only load case I, Eqs. (2a).

The geometry is an isotropic geometry (as in [25]) with the delamination parallel to the shell reference surface and extending along the entire length of the panel. Moreover, the panel is assumed to be very long and thus the solution is not affected by the x=constant boundary conditions. Finally, the boundaries at θ = const. are taken to be clamped.

The results are used to study the effect of delamination position (through the thickness), $\bar{h}$, and of delamination size, α (see Fig. 1). Note that the results correspond to $\beta = \gamma$ for the case of panels.

The results are presented both in tabular and graphical form, for a complete circular shell as well as for panels of angle π and $\pi/2$. Critical load parameter values, $-\lambda$ ($\lambda = qR^3/D$), are shown in Tables 1-3 for various values of α and $\bar{h}$. The mode is either symmetric (S) or antisymmetric (A), and it is designated as such in the tables and on the figures, Figs. 2-4.

For the complete cylindrical shell, and for midsurface delamination $\bar{h} = 0.5$, the critical load parameter is 3 for the perfect configuration, and it decreases to 0.75 when the delamination extends to the entire circumference. It is next shown that this is a reasonable expectation.

It is assumed that before buckling the circularity is maintained, there is complete contact of parts I and II (see Fig. 1), and if one denotes by q^I, q^{II}, q^{III} and q^{IV} the pressures on the various parts then

$$q^{III} = q^{IV} = q$$

$$\text{and } q^I = q - q^{II}. \tag{30}$$

Moreover, in the primary state

$$w^j = \frac{R_j^2 q^j}{E h^j} \qquad j = \text{I, II, III and IV,}$$

$$w^I = w^{II} = w^{III} = w^{IV}, \qquad \text{and } R^j = R \tag{31}$$

Then, before and up to the instant of buckling the pressure loadings on parts I and II, q^I and q^{II}, are related to the applied loading q, through Eqs. (31), by

$$q^I = \bar{h}\, q \quad ; \quad q^{II} = (1 - \bar{h})\, q \tag{32}$$

If λ^j is defined as

$$\lambda^j = q^j R^3 / D^j \qquad j = \text{I, II, III, and IV} \tag{33}$$

then

$$\lambda^{III} = \lambda^{IV} = q\, R^3/D = \lambda$$

$$\lambda^I = q^I R^3/D^I = (\bar{h} q\, R^3/D^I)\, \frac{D}{D} = \frac{\lambda}{\bar{h}^2} \tag{34}$$

$$\lambda^{II} = q^{II} R^3/D^{II} = \lambda/(1-\bar{h})^2$$

Clearly then, when the cylindrical shell is completely delaminated

$$\lambda_{cr} = \bar{h}^2 \lambda^I_{cr}$$

and $\lambda^I_{cr} = -3.0$; therefore $\lambda_{cr} = -0.75$ for $\bar{h} = 0.5$.

One may say at this point that the residual strength of the completely delaminated thin cylindrical shell is equal to

$$\lambda_{total} = [\bar{h}^2 + (1-\bar{h})^2](-3)$$

Thus, for $\bar{h} = 0.5$ $\lambda_{total} = -1.5$, while for $\bar{h} = 0.1$

$$\lambda_{total} = 0.82(-3) = -2.46.$$

The results corresponding to the complete thin delaminated cylinder are shown in Table 1. Note that when $\alpha = 6.2$ (close to 2π) the value of the buckling load parameter is $(0.1)^2$ (3) or 0.0003. The same results are presented graphically on Fig. 2, while Fig. 3 shows the complete curves corresponding to symmetric and antisymmetric buckling but only for $\bar{h} = 0.5$.

Furthermore, there exists two important observations. One is that the critical load associated with the very small $\bar{h}$-values should be viewed as measures of local buckling and not as measures of load bearing capacity of the overall structure [25]. The second observation is that in most cases the buckling mode of the two parts that are separated by the delamination (parts I and II ; see Fig. 1), is an antisymmetric mode of the type that suggests contact over a certain portion and no contact over the remaining one. This suggests that the postbuckling behavior for shells with $\bar{h}$ will be different from that of shells with $(1 - \bar{h})$, although the critical loads are the same for the two (see Table 1). Moreover, for each geometry, regardless of $\bar{h}$, the transition from buckling to postbuckling behavior will require accommodation of the predicted (buckling mode) contact.

Results for clamped panels with $\phi = \pi$ and $\pi/2$ and symmetric delamination ($\beta = \gamma$) are presented in Tables 2 and 3 and on Figs. 4 and 5. All generated results correspond to an antisymmetric mode. For these results also, as in the case of the complete cylinder, the critical load varies from the perfect geometry critical load [34,35], when α is very small, to the value of $\bar{h}^2 \lambda_{perf.}$ [or $(1-\bar{h})^2 \lambda_{perf.}$], when the panel is completely delaminated (see Fig. 1).

From the above results it is clear that further and more detailed studies need be performed before we fully understand the complex response of delaminated, curved laminates.

Acknowledgement: This work is partially supported by the United States Air Force Office of Scientific Research under Grant No. AFOSR-86-0038. This financial support is gratefully acknowledged.

References

1. Tennyson, R. C., "Buckling of Laminated Composite Cylinders: Review", Composites, Jan., 1975, pp. 17-24.

2. Hirano, Y., "Buckling of Angle-Ply Laminated Circular Cylindrical Shells", Journal of Applied Mechanics, v. 46, pp. 233-234, 1979.

3. Semenyuk, N. P., and Zhukova, N. B., "Stability of Three-Layered Cylindrical Shells with a Discrete Filler in Axial Compression", Soviet Applied Mechanics, v. 19, No. 3, 1983, pp. 222-226.

4. Babich, I. Y., Guz', A. N., and Deriglazov, L. V., "Stability of Triple-layer Anisotropic Cylindrical Shells", Soviet Applied Mechanics, v. 19, No. 9, 1984, pp. 753-758.

5. Troshina, L. A., "Stability of Triple-layer Cylindrical Shells with Dissymmetry and with Nonrigic Filter under Axial Compression", Mekhanika Kompozitnykh Materialov, No. 3, 1983, p.472-475.

6. Rao, K. M., "Buckling Analysis of FRP-faced Anisotropic Cylindrical Sandwich Panel", J. Eng. Mech., Vol. 111, No. 4, 1985, pp. 529-544.

7. Simitses, G. J., Sheinman, I., and Shaw, D., "Stability of Laminated Composite Shells Subjected to Uniform Axial Compression", AFOSR-TR-82-XXXX (written under Grant AFOSR-81-0227) Ga. Tech., Atlanta, Ga., 1982.

8. Sheinman, I., Shaw, D. and Simitses, G. J., "Nonlinear Analysis of Axially-loaded Laminated Cylindrical Shells", Computers and Structures, v. 16, No. 1-4, 1983, pp. 131-137.

9. Shaw, D., Simitses, G. J. and Sheinman, I., "Imperfect, Laminated, Cylindrical Shells in Torsion and Axial Compression", Acta Astronautica, v. 10, No. 5-6, 1983, pp. 395-400.

10. Simitses, G. J., Sheinman, I., and Shaw, D., "Analysis of the Nonlinear Large Deformation Behavior of Composite Cylindrical Shells", AFOSR-TR-83-XXX (written under Grant AFOSR-81-0227) Ga Tech., Atlanta, Ga. 1982.

11. Zhang, Y., and Matthews, F. L., "Initial Buckling of Curved Panels of Generally Layered Composite Materials, Composite Structures, Vol. 1, No. 1, 1983, pp. 3-30.

12. Zhang, Y., and Matthews, F. L., "Postbuckling Behavior of Curved Panels of Generally Layered Composite Materials", Composite Structures, Vol. 1, No. 2, 1983, pp. 115-135.

13. Whitney, J. M., "Buckling of Anisotropic Laminated Cylindrical Plates", AIAA Journal, Vol. 22, No. 11, 1984, pp. 1641-1645.

14. Hui, D., "Asymmetric Postbuckling of Symmetrically Laminated Cross-Ply Short Cylindrical Panels under Compression", Composite Structures, Vol. 3, 1985, pp. 81-95.

15. Whitcomb, J. D., "Finite Element Analysis of Instability Related Delamination Growth", J. Composite Materials, Vol. 15, 1981, pp. 403-426.

16. Shivakumar, K. N., and Whitcomb, J. D., "Buckling of a Sublaminate in a Quasi-Isotropic Composite Laminate", J. Composite Materials, Vol. 19, 1985, pp. 2-18.

17. Yin, W. L., and Wang, J. T. S., "Postbuckling Growth of a One-Dimensional Delamination. Part I - Evaluation of the Energy Release Rate", J. Appl. Mechanics, Vol. 51, No. 4, 1984, pp. 939-941.

18. Yin, W. L. and Fei, Z. Z., "Buckling Load of a Circular Plate with a Concentric Delamination", Mechanics Research Communications, Vol. 11, No. 5, 1984, pp. 337-344.

19. Gillespie, Jr., J. W., and Pipes, R. B., "Compressive Strength of Composite Laminates with Interlaminar Defects" Composite Structures, Vol. 2, 1984, pp. 49-69.

20. Wang, S. S., "Edge Delamination in Angle-Ply Composite Laminates", AIAA Journal, V. 22, No. 2, 1984, pp. 256-264.

21. Chai, Herzl, and Babcock, C. D., "Two-Dimensional Modelling of Compressive Failure in Delaminated Laminates", J. Composite Materials, v. 19, 1985, pp. 67-98.

22. Simitses, G. J., and Sallem, S. and Yin, W. L., "Effect of Delamination of Axially Loaded Homogeneous Laminated Plates", AIAA Journal, Vol. 23, No. 9, 1985, pp. 1437-1444.

23. Simitses, G. J. and Sallam, S., "Delamination Buckling and Growth of Flat Composite Structural Elements", AFOSR-TR-84-XXXX (written under Grant AFOSR 83-0243) Ga. Tech, Atlanta, Ga., 1984.

24. Yin, W. L., Sallem, S. N. and Simitses, G. J., "Ultimate Axial Load Capacity of a Delaminated Beam-Plate", AIAA J., Vol. 24, No. 1, 1986, pp. 123-129.

25. Troshin, V. P., "Effect of Longitudinal Delamination in a Laminar Cylindrical Shell on the Critical External Pressure", Mechanics of Composite Materials, v. 17, No. 5, 1983, pp. 563-567.

26. Troshin, V. P., "Use of Three-Dimensional Model of Filler in Stability Problems for Triple-Layer Shells with Delaminations", Mekhanika Kompozitnykh Materialov, No. 4, 1983, pp. 657-662.

27. Sallam, S. and Simitses, G. J., "Delamination Buckling of Cylindrical Shells Under Axial Compression", Composite Structures, in print, 1986.

28. Budiansky, B., "Notes on Nonlinear Shell Theory", Journal of Applied Mechanics, Vol. 35, No. 2, June 1968. pp. 393-401.

29. Sanders, J. L., "Nonlinear Theories of Thin Shells", Quarterly of Applied Mathematics, Vol. 21, 1963, pp. 21-36.

30. Simitses, G. J., and Aswani, M., "Buckling of Thin Cylinders Under Uniform Lateral Loading", Journal of Applied Mechanics, Vol. 41, No. 3, Sept. 1974, pp. 827-829.

31. Wempner, G. A., and Kesti, N. E., "On the Buckling of Circular Arches and Rings", Proceedings , 4th U.S. National Congress of Applied Mechanics, Vol. 2, 1962, pp. 843-849.

32. Jones, R. M., Mechanics of Composite Materials, McGraw-Hill Book Co., New York, 1975.

33. Hoff, N. J., "The Perplexing Behavior of Thin Circular Cylindrical Shells in Axial Compression:, Israel Journal of Techn., Vol. 4, No. 1, 1966, pp. 1-28.

34. Simitses, G. J., Elastic Stability of Structures, Prentice-Hall, Inc., Englewood Cliffs, N. J., 1976.

35. Timoshenko, S. P., and Gere, J. M., Theory of Elastic Stability, McGraw-Hill Book Co., Inc., New York, 1961.

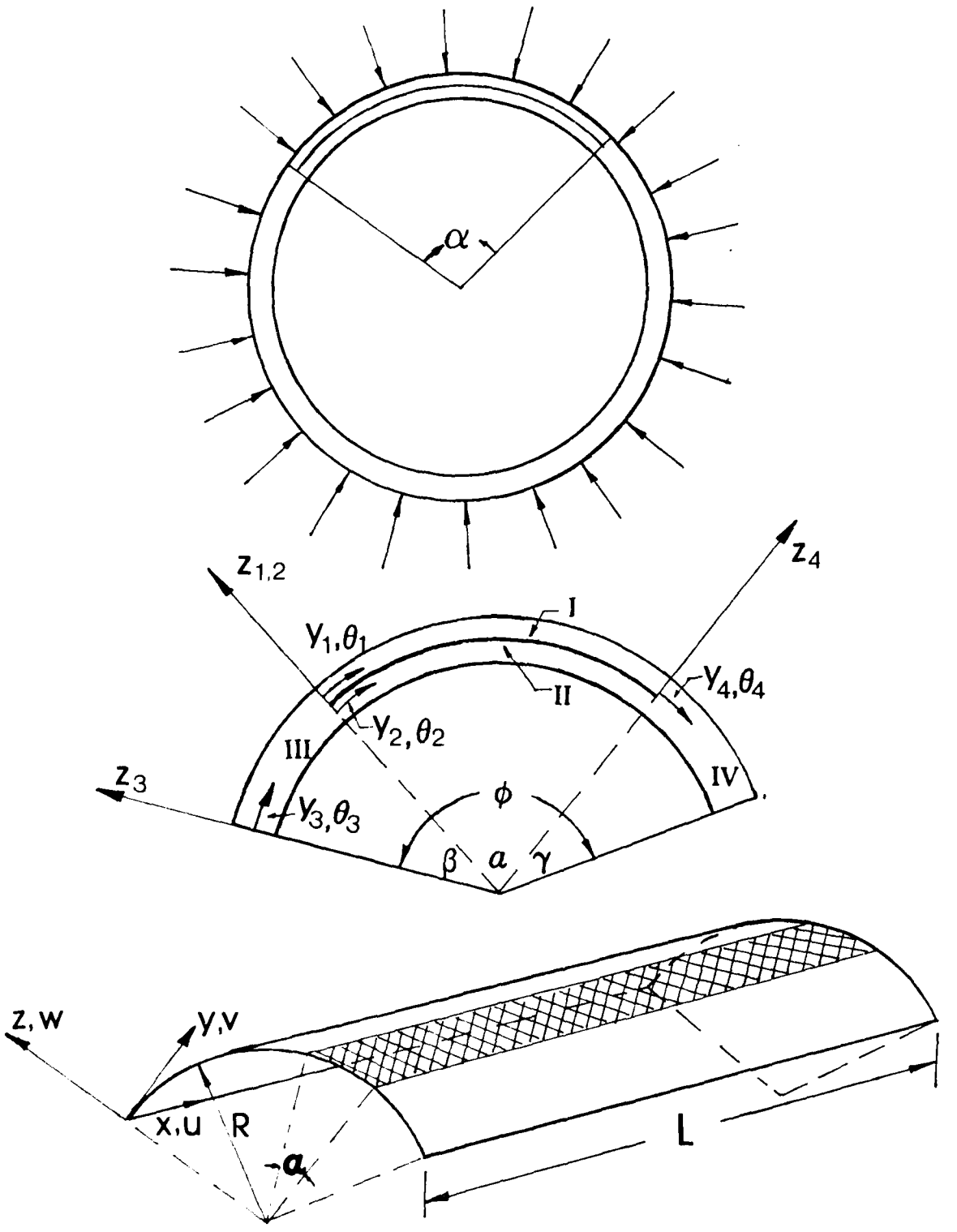

Fig. 1. Geometry, Loading and Sign Convention

Table 1 Buckling Load for a Delaminated Circular Cylindrical Shell

α \ $\bar{h}$	0.5	0.3(0.7)	0.1(0.9)	0.01(0.99)
0.000	3.00000(A)	3.00000(A)	3.00000(A)	3.00000(A)
0.2	2.88461(S)	2.86341(S)	2.93602(S)	0.20186(A)
0.4	2.41778(S)	2.57496(S)	2.87696(S)	0.05044(A)
0.6	2.27045(S)	2.46545(S)	2.23770(A)	0.02240(A)
0.8	2.23305(S)	2.42099(S)	1.25739(A)	0.01260(A)
1.0	2.19743(A)	2.40772(S)	0.80364(A)	0.00803(A)
1.2	1.94698(A)	2.31670(A)	0.55715(A)	0.00557(A)
1.4	1.76893(A)	2.12619(A)	0.40858(A)	0.00408(A)
1.6	1.65424(A)	1.95652(A)	0.31218(A)	0.00312(A)
1.8	1.58796(A)	1.78177(A)	0.24614(A)	0.00246(A)
2.0	1.55616(A)	1.57452(A)	0.19894(A)	0.00199(A)
2.2	1.54597(A)	1.35834(A)	0.16406(A)	0.00164(A)
2.4	1.50758(S)	1.16633(A)	0.13757(A)	0.00137(A)
2.6	1.38708(S)	1.00618(A)	0.11701(A)	0.00117(A)
2.8	1.29118(S)	0.87462(A)	0.10075(A)	0.00101(A)
3.0	1.21859(S)	0.76648(A)	0.08769(A)	0.00088(A)
3.2	1.16706(S)	0.67713(A)	0.07706(A)	0.00077(A)
3.4	1.13386(S)	0.60284(A)	0.06832(A)	0.00068(A)
3.6	1.11579(S)	0.54070(A)	0.06107(A)	0.00061(A)
3.8	1.10883(S)	0.48847(A)	0.05501(A)	0.00055(A)
4.0	1.10645(S)	0.44445(A)	0.04993(A)	0.00050(A)
4.2	1.03733(A)	0.40729(A)	0.04566(A)	0.00046(A)
4.4	0.97570(A)	0.37596(A)	0.04207(A)	0.00042(A)
4.6	0.92187(A)	0.34970(A)	0.03907(A)	0.00039(A)
4.8	0.87585(A)	0.32788(A)	0.03658(A)	0.00037(A)
5.0	0.83751(A)	0.31006(A)	0.03455(A)	0.00035(A)
5.2	0.80665(A)	0.29590(A)	0.03294(A)	0.00033(A)
5.4	0.78308(A)	0.28514(A)	0.03172(A)	0.00032(A)
5.6	0.76645(A)	0.27756(A)	0.03086(A)	0.00031(A)
5.8	0.75620(A)	0.27287(A)	0.03032(A)	0.00030(A)
6.0	0.75131(A)	0.27061(A)	0.03007(A)	0.00030(A)
6.2	0.75003(A)	0.27002(A)	0.03000(A)	0.00030(A)

(S) SYMM. Buckling Mode
(A) ANTI-SYMM. Buckling Mode

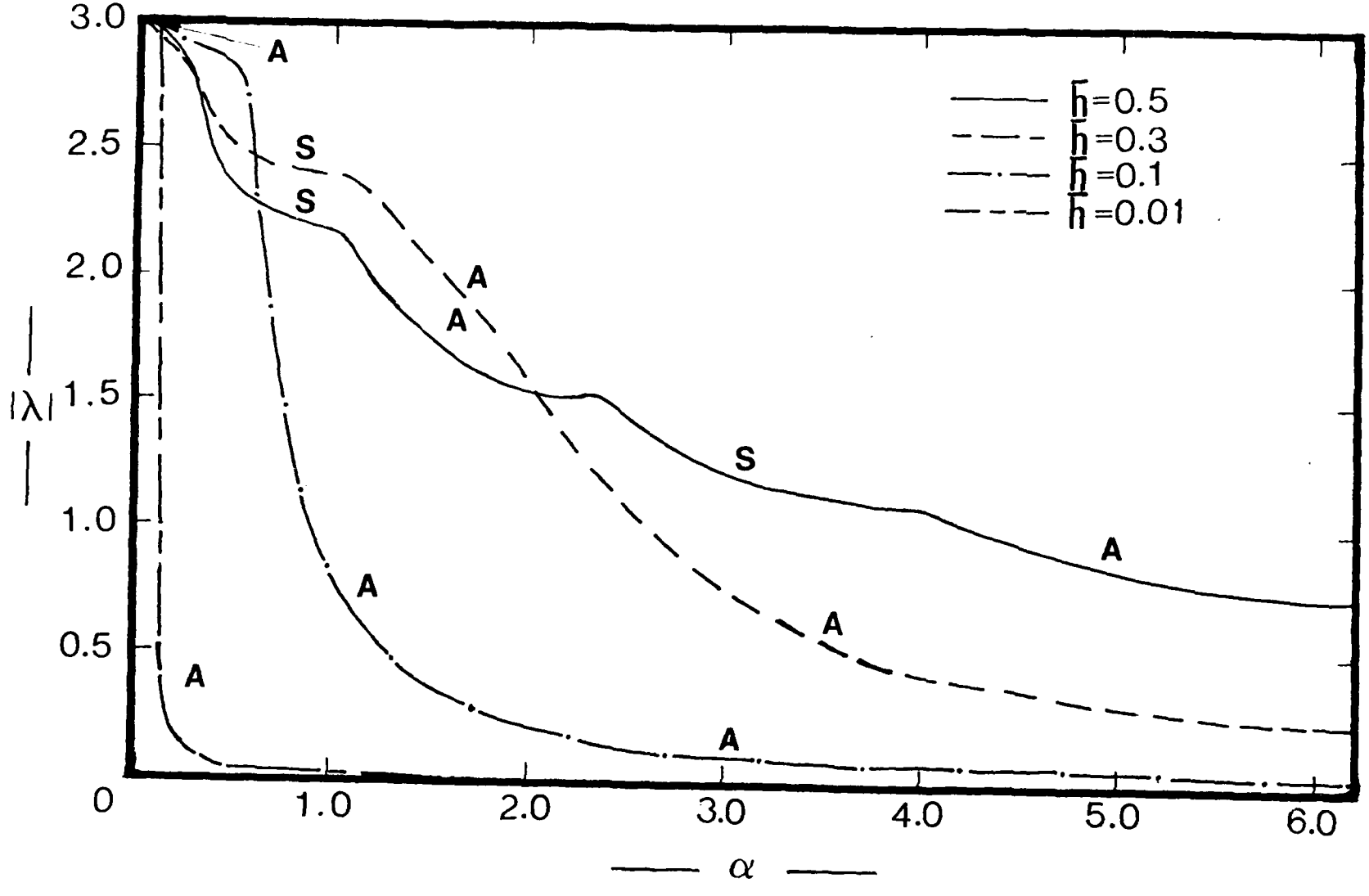

Fig. 2. Critical Loads for a Long, Thin, Cylindrical Shell.

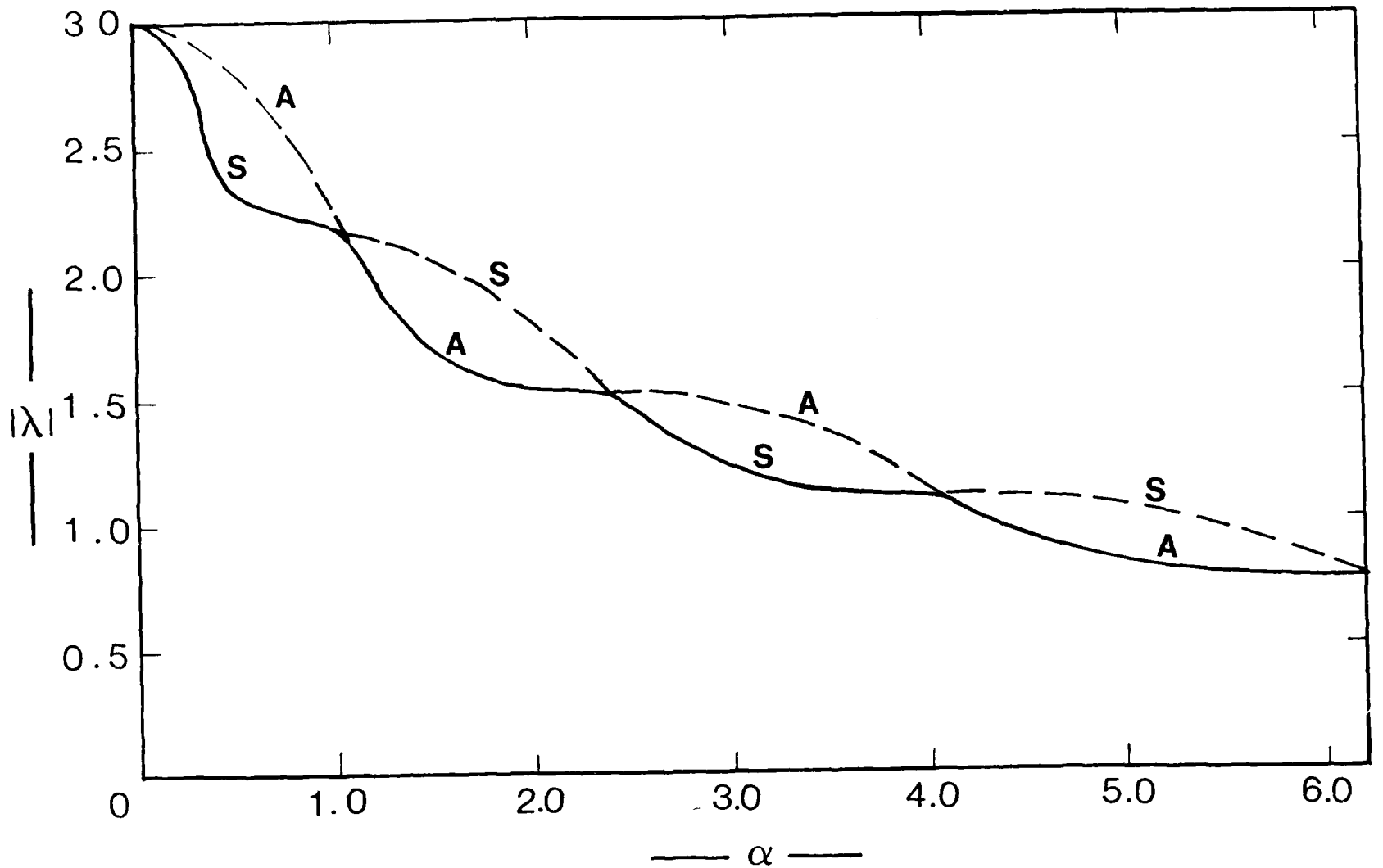

Fig. 3. Symmetric and Antisymmetric Critical Loads for the Cylindrical Shell with Midsurface Delamination ($\bar{h}$= 0.5).

Table 2 Buckling Load for a Delaminated Panel of Angle π (rad.)
(Clamped Boundaries)

α \ $\bar{h}$	0.5	0.3(0.7)	0.1(0.9)	0.01(0.99)
0.000	8.00000(A)	8.00000(A)	8.00000(A)	8.00000(A)
0.2	7.90294(A)	7.94443(A)	7.98782(A)	0.20187(A)
0.4	7.18972(A)	7.56860(A)	5.03907(A)	0.05044(A)
0.6	5.81200(A)	6.71586(A)	2.23788(A)	0.02240(A)
0.8	4.64551(A)	5.71862(A)	1.25744(A)	0.01258(A)
1.0	3.94345(A)	4.86852(A)	0.80366(A)	0.00804(A)
1.2	3.58022(A)	4.10046(A)	0.55720(A)	0.00557(A)
1.4	3.43175(A)	3.31777(A)	0.40862(A)	0.00409(A)
1.6	3.40141(A)	2.63529(A)	0.31223(A)	0.00312(A)
1.8	3.39324(A)	2.12076(A)	0.24619(A)	0.00246(A)
2.0	3.31556(A)	1.73589(A)	0.19898(A)	0.00199(A)
2.2	3.13397(A)	1.44421(A)	0.16410(A)	0.00164(A)
2.4	2.88519(A)	1.21911(A)	0.13762(A)	0.00138(A)
2.6	2.61981(A)	1.04247(A)	0.11706(A)	0.00117(A)
2.8	2.36815(A)	0.90161(A)	0.10080(A)	0.00101(A)
3.0	2.14240(A)	0.78775(A)	0.08774(A)	0.00088(A)
3.141	2.00056(A)	0.72026(A)	0.08003(A)	0.00080(A)

(S) SYMM. Buckling Mode

(A) ANTI-SYMM. Buckling Mode

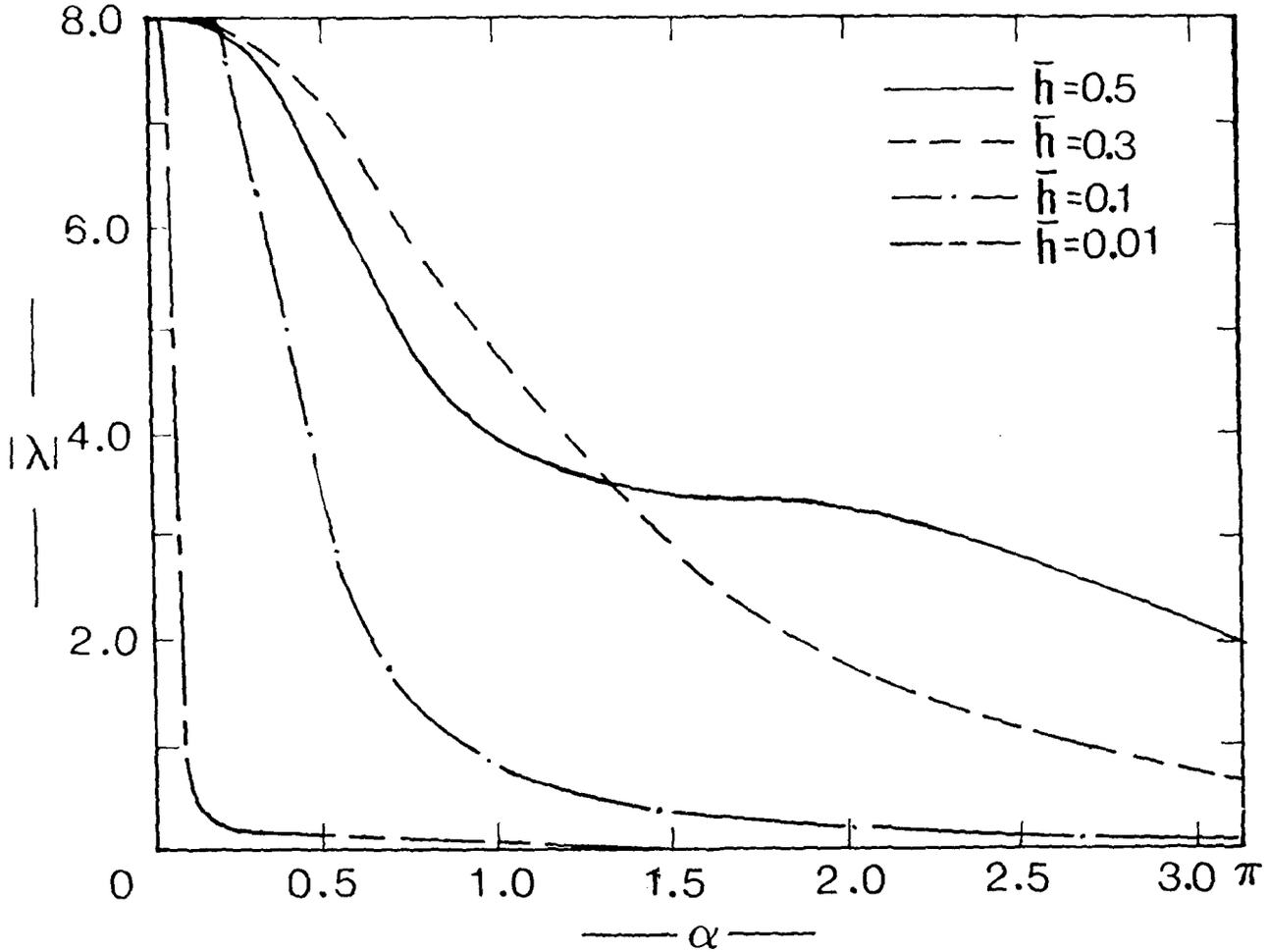

Fig. 4. Critical Loads for a Long, Thin, Clamped, Cylindrical Panel of Angle π.

Table 3 Buckling Load for a Delaminated Panel of angle $\pi/2$(rad.)
(Clamped Boundaries)

α \ $\bar{h}$	0.5	0.3(0.7)	0.1(0.9)	0.01(0.99)
0.000	32.59514(A)	32.49695(A)	32.43374(A)	32.43112(A)
0.2	29.21156(A)	30.70972(A)	20.16636(A)	0.20186(A)
0.4	18.67281(A)	23.12066(A)	5.03951(A)	0.05044(A)
0.6	13.92583(A)	16.33205(A)	2.23812(A)	0.02240(A)
0.8	12.87370(A)	10.54976(A)	1.25768(A)	0.01258(A)
1.0	12.72554(A)	6.99228(A)	0.80391(A)	0.00803(A)
1.2	11.46249(A)	4.93227(A)	0.55745(A)	0.00558(A)
1.4	9.57106(A)	3.65625(A)	0.40889(A)	0.00409(A)
1.57	8.11394(A)	2.92168(A)	0.32464(A)	0.00325(A)

(S) SYMM. Buckling Mode

(A) ANTI-SYMM. Buckling Mode

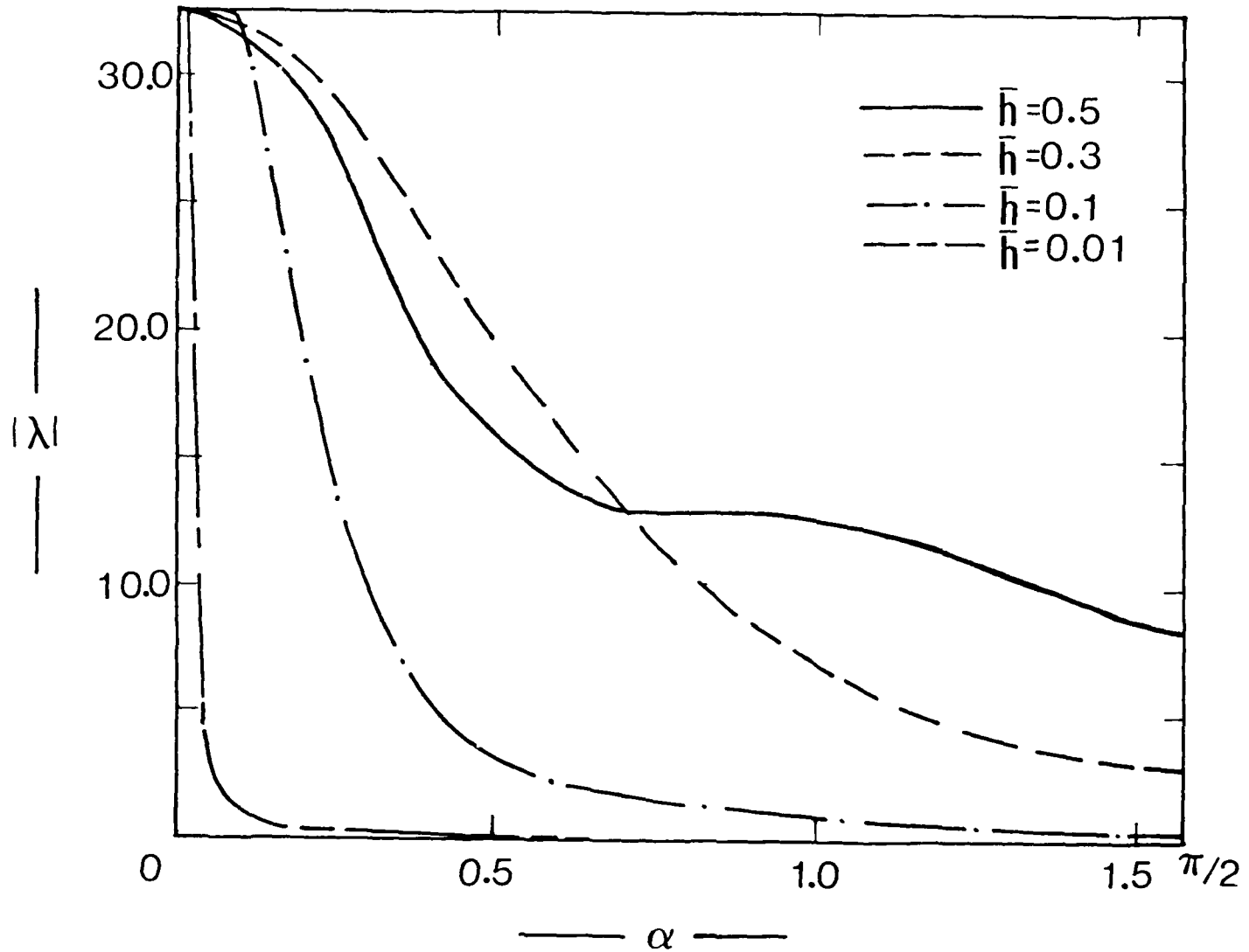

Fig. 5. Critical Loads for a Long, Thin, Clamped, Cylindrical Panel of Angle $\pi/2$.

PART B. BUCKLING OF ANNULAR PLATES

EFFECT OF BOUNDARY CONDITIONS AND RIGIDITIES ON THE BUCKLING OF ANNULAR PLATES

G. J. Simitses and Y. Frostig

Engineering Science and Mechanics
Georgia Institute of Technology, Atlanta, GA. 30332

ABSTRACT

The buckling analysis of multi-annular plates, with different properties, is presented. The geometry may include ring stiffeners at the common joints and the plate may be supported in various manners, simple supports, clamped supports, etc., at the loaded outer edge. The loading is uniform radial compression and static. Several parametric studies are performed in order to assess the effect of geometry, material properties of the annular sections and of the ring stiffness. Moreover, when rings are present, the ring geometry is modelled both as a curved beam and as an annular plate, for comparison purposes.

INTRODUCTION

The stability of multi-annular plates with or without ring stiffeners is being considered. Most researchers have investigated the buckling of a single annular plate (with or without a rigid inclusion) when subjected to, primarily, a uniform stress field.

Several studies [1-8] nave been reported in the open literature for circular and/or annular plates under various loads, boundary conditions and thickness variation; see also their cited references.

Moreover, a few studies report on stiffened configurations with special stiffening [4,9,10].

In all of the above studies, certain simplifying assumptions were made, such as neglecting the extensional stiffness of the ring stiffeners [10], which may or may not have a significant effect on the critical load. Moreover, the annular sections were considered to be homogeneous and of the same material, by virtually all investigators.

The present manuscript deals with buckling of multi-annular plates with different material properties and thickness and stiffened or

unstiffened by rings at the common joints. The inplane loading is axisymmetric and several combinations of transverse and inplane boundary conditions are considered. The mathematical modeling accounts for the extensional rigidity of the rings, in addition to their torsional and bending stiffnesses.

MATHEMATICAL FORMULATION

The equations governing the primary state for each part are; (see [11]).

$$\begin{aligned} (rN^{o}_{rr})_{,r} - N_{\theta\theta} &= 0 \\ N^{o}_{\theta\theta,\theta} &= 0 \end{aligned} \tag{1}$$

The buckling equation for each part of the plate is:

$$D\nabla^4 w = N^{o}_{rr} w_{,rr} + N^{o}_{\theta\theta} \left(\frac{w_{,\theta\theta}}{r^2} + \frac{w_{,r}}{r} \right) \tag{2}$$

where N^{o}_{rr}, $N^{o}_{\theta\theta}$ are primary state stress resultants in the radial and circumferential directions, respectively; w is the transverse displacement; $(\ )_{,r}(\ )_{,\theta}$ are partial derivatives with respect to radial or angular coordinates and D is the flexural rigidity. The geometry and loading are shown on figure 1.

The inplane stress resultant distribution is solved first, using equations (1). The constants are determined through continuity conditions at the common joints, see [11]. In case of a stiffened plate, the continuity conditions include the deformation and radial stress resultants of the stiffener (see [12]).

The inplane stress distribution in the various parts of the plate depends on the extensional rigidity of the various parts, in addition to

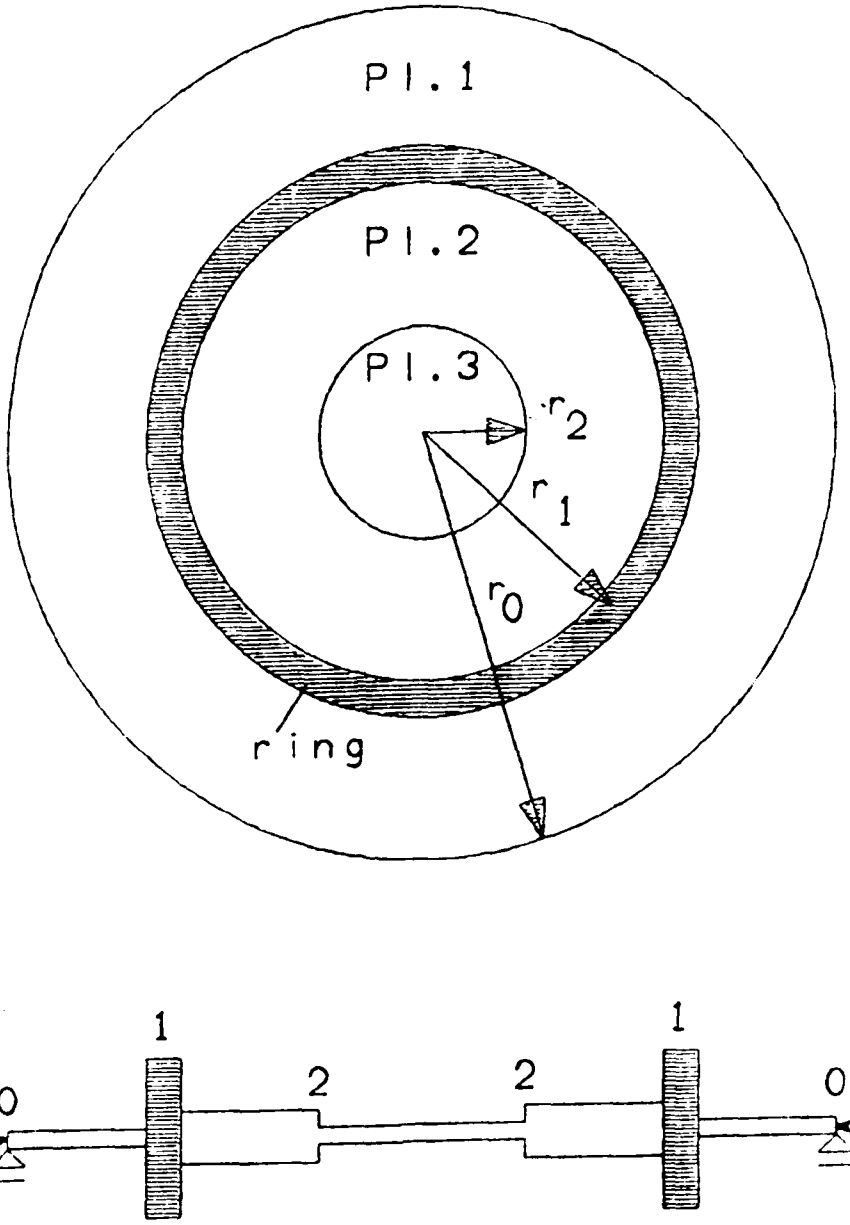

Fig. 1. Geometry and cross section of ring stiffened multi-annular plate

the extensional rigidity of the stiffener. Even in cases where the plate is homogeneous, but with stiffeners, the stress distribution is not constant as suggested by Rossettos [10]. The exact distribution depends on the extensional rigidity and location of stiffeners. The buckling equation for each part is given by equation (2). The equation is solved by assuming a separable solution of the form:

$$w(r,\theta) = \sum_{n=0}^{\infty} F_n(r) \cos n\theta \qquad (3)$$

where $F_n(r)$ is the deflection function in the r direction for the nth buckling mode.

The constants for the transverse deflection are calculated using continuity and equilibrium conditions at the common joints and boundary conditions at the edges; see [11] for the unstiffened plate. In the case of a stiffened plate the continuity conditions are applied also to the stiffener. The equilibrium conditions include the contributions of the stiffener, related to their bending and torsional rigidities; see [12].

In the case of a plate with a ring of rectangular cross-section, it is possible to analyze it by considering the entire system as a multi-annnuilar plate. In such a case the dimensions of the rectangular ring must be such that plate theory is applicable to all plate segments (inner, ring and outer). Here, the various ring stiffnesses can be expressed in terms of the ring plate material properties (E_R, ν_R) and thickness t_R. In this case, if the bending rigidity is fixed, the torsional rigidity is also fixed (depending only on the Poisson's ratio).

A numerical example is presented in a subsequent section and the results are compared with those based on ring-stiffened plate analysis.

NUMERICAL EXAMPLES

A computer program has been developed, and it is described with sufficient detail in [11]. With the aid of this program several parametric studies are performed. The results consist of critical loads, corresponding to axisymmetric (n = 0) and asymmetric (n = 1) buckling modes, for multi-annular plates. The geometry is a two part plate, one annular and one circular, with different material properteis, with or without a single ring stiffener, located either at the edges or at the common joint.

The stiffener rigidities are expressed in a non-dimensional form as follows:

$$\alpha_R = \frac{EA_R}{E_1 t_1 (1 - \nu_1^2)\, r_o} \quad ; \quad \beta_R = \frac{EI_R}{E_1 t_1^3/12\, (1 - \nu_1^2)\, r_o}$$

$$\gamma_R = GJ_R / EI_R \tag{4}$$

where, EA_R, EI_R, GJ_R are the extensional, flexural and torsional rigidities of the ring, respectively. E_1, t_1, ν_1 are the modulus of elasticity, thickness and Poisson's ratio, respectively, for the outer plate, and r_o is the outer radius of plate.

Before discussing the numerical results, we present the influence of the extensional rigidites of the various sections, including the one of the stiffener, on the distribution of the primary (prebuckling) stress resultant, N^o_{rr}.

Primary State Distributions

The primary state is solved for first, by equations (1). The presence of a stiffener, because of its extensional rigidity, influences the stress distributions. The parameters to be considered are the ratio of the moduli, E_2/E_1, the stiffener rigidity, α_R, and the position of common joint, r_1/r_o.

The constant stress resultant of the inner plate is derived analytically, by using equations (1) and the continuity conditions.

$$N^o_{rr_2} = \frac{\left(\frac{E_2}{E_1}\right)\left(\frac{u_1}{u_o}\right)(\beta_1^2 - 1)(1 + \nu)}{\left[-(1 + \nu)\beta_1 - \frac{1 - \nu}{\beta_1} + 2\left(\frac{u_1}{u_o}\right)\right]} \bar{N}_{rr} \qquad (5)$$

where $u_1/u_o = 2\beta_1 / \left[(1 + \nu) + \beta_1^2 (1 - \nu) + (E_2/E_1)(1 + \nu)(\beta_1^2 - 1) + \right.$

$$\left. + \alpha_R \beta_1 (\beta_1^2 - 1)\right] \quad ; \qquad \beta_1^2 = r_o/r_1; \qquad (6)$$

ν - Poisson's ratio of the plates ($\nu_1 = \nu_2 = \nu$) ; and $\bar{N}_{rr} = \frac{k D_o}{r_o^2}$, applied at the outer edge.

In case of a plate stiffened by an edge ring, the constant stress resultant of the inner part becomes

$$N^o_{rr_2} = - N_{rr} / \left[1 + \alpha_R E_1/E_2 (1 + \nu)\right] \qquad (7)$$

The effect of the stiffener extensional rigidity on the stress resultant distribution of an annular plate, stiffened by a single ring at the inner edge, appears on figure 2. As α_R is increased the stress

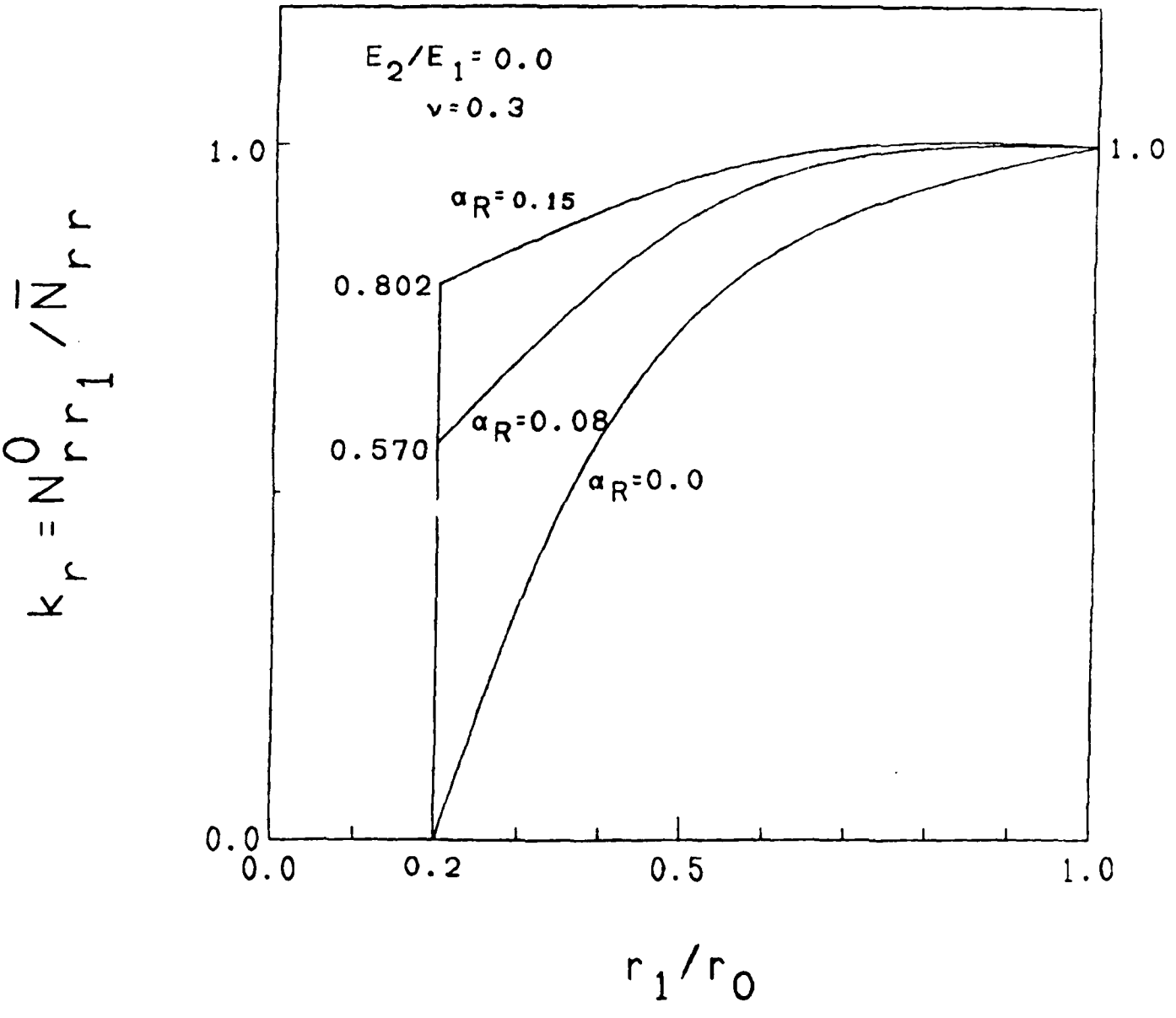

Fig. 2. Primary radial stress distribution of a stiffened annular plate ($r_1/r_0 = 0.2$).

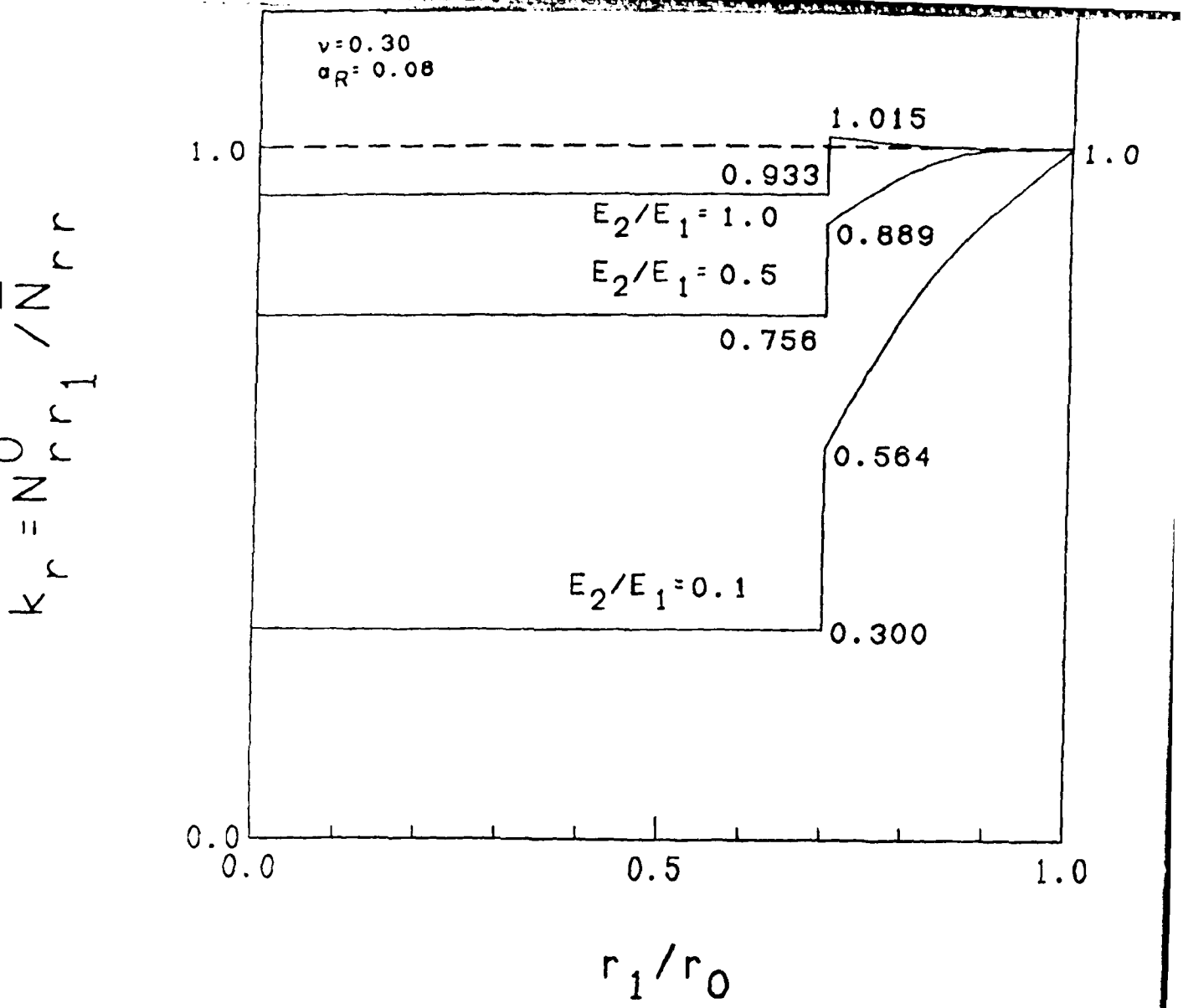

Fig. 3. Stress distribution, N^o_{rr} of ring-stiffened two part plate. (r_1/r_o = 0.7).

resultant increases throughout the annular plate. Note that if there is no ring ($\alpha_R = 0$), the radial stress resultant is zero and increases (parabolically) to the value of the applied loading, N_{rr}. When $\alpha_R \neq 0$, because of the presence of the ring, the value of N^o_{rr} close to the stiffener is greater than zero and its variation with position (r/r_o) is the same as before.

In the case of a multi-annular plate, stiffened by a ring, the stress resultant distribution depends on α_R and ring position r_1/r_o, but also on the stiffnesses of the two plate sections, E_2/E_1. Figure 3 describes the stress distribution for a two-part plate stiffened by a ring at the common joint (taken as $r_1/r_o = 0.7$). The ring extensional stiffness parameter is taken as $\alpha_R = 0.05$ (corresponding to light stiffening [12]) and $E_2/E_1 =$ 0.1, 0.5 and 1.0. Note that for $E_2/E_1 = 1.0$, the stress resultant increases as we move towards the ring, then there is a drop (because of the extensional stiffness of the ring), and finally it becomes constant for the inner part. For $E_2/E_1 = 0.5$ and 0.1, the only difference is that the stress resultant distribution decreases (outer annular section) as we move towards the ring.

Simply-supported Multi-annular Plates

The two-part plate is simply-supported and loaded by a radial axisymmetric in-plane loading at the outer edge. The case of a stiffened configuration, with a single ring located at the common joint, is also considered.

Critical loads are calculated for the following parameters:

$\nu = \nu_1 = \nu_2 = 1/3$; $n = 0, 1$ (modes); $t_1 = t_2$;

$E_2/E_1 = 0$ (hole), 0.01, 0.1, 0.5, 1.0;

and $r_1/r_o = 0.0, 0.1 \ldots\ldots\ldots 0.9, 1.0$.

For the stiffened configuration the following parameters are considered:

$n = 0$; $\alpha_R = 0.08$; $\beta_R = 1.2$ (axisym.)

$n = 1$; $\alpha_R = 0.08$; $\beta_R = 1.2$; $\gamma_R = 0.6$ (asym.)

Note that the torsional ring stiffness, γ_R, does not affect axisymmetric ($n = 0$) buckling.

The results for the unstiffened plate appear on figure 4 for the axisymmetric buckling mode. For the same mode, the results for the stiffened configuration appear on figure 5. Figures 6 and 7 describe the results, corresponding to the asymmetric mode ($n = 1$), for unstiffened and stiffened plates, respectively.

The following conclusions can be drawn from these figures:

1) The critical load (lowest eigenvalue) corresponds to the axisymmetric mode, for both types of plates.

2) The buckling load for an unstiffened plate is decreasing as the ratio of the radii increases., This is true for both modes. In the stiffened case, figure 5, the critical load increases with r_1/r_o, for $r_1/r_o \leq 0.7$, and then it decreases, for $r_1/r_o \geq 0.7$. For a stiffened annular plate, $E_2/E_1 = 0$, the critical load increases continuously with increasing r_1/r_o.

3) For a two-part unstiffened plate ($0 \leq E_2/E_1 \leq 1.0$), the critical load depends on E_2/E_1 and r_1/r_o. For extremely small values of E_2/E_1 (it is observed for values of 0.1 and 0.01, and the observation probably is true for E_2/E_1 values in the range of $0.1 < E_2/E_1 < 0.5$ the behavior depends on the ratio of the radii (r_1/r_o). For $E_2/E_1 = 0.1$, as long as r_1/r_o is smaller than approximately 0.55, buckling seems to be triggered mainly by the annular part and the critical load is a little larger than corresponding to $E_2/E_1 = 0$ (pure annular plate). On the other

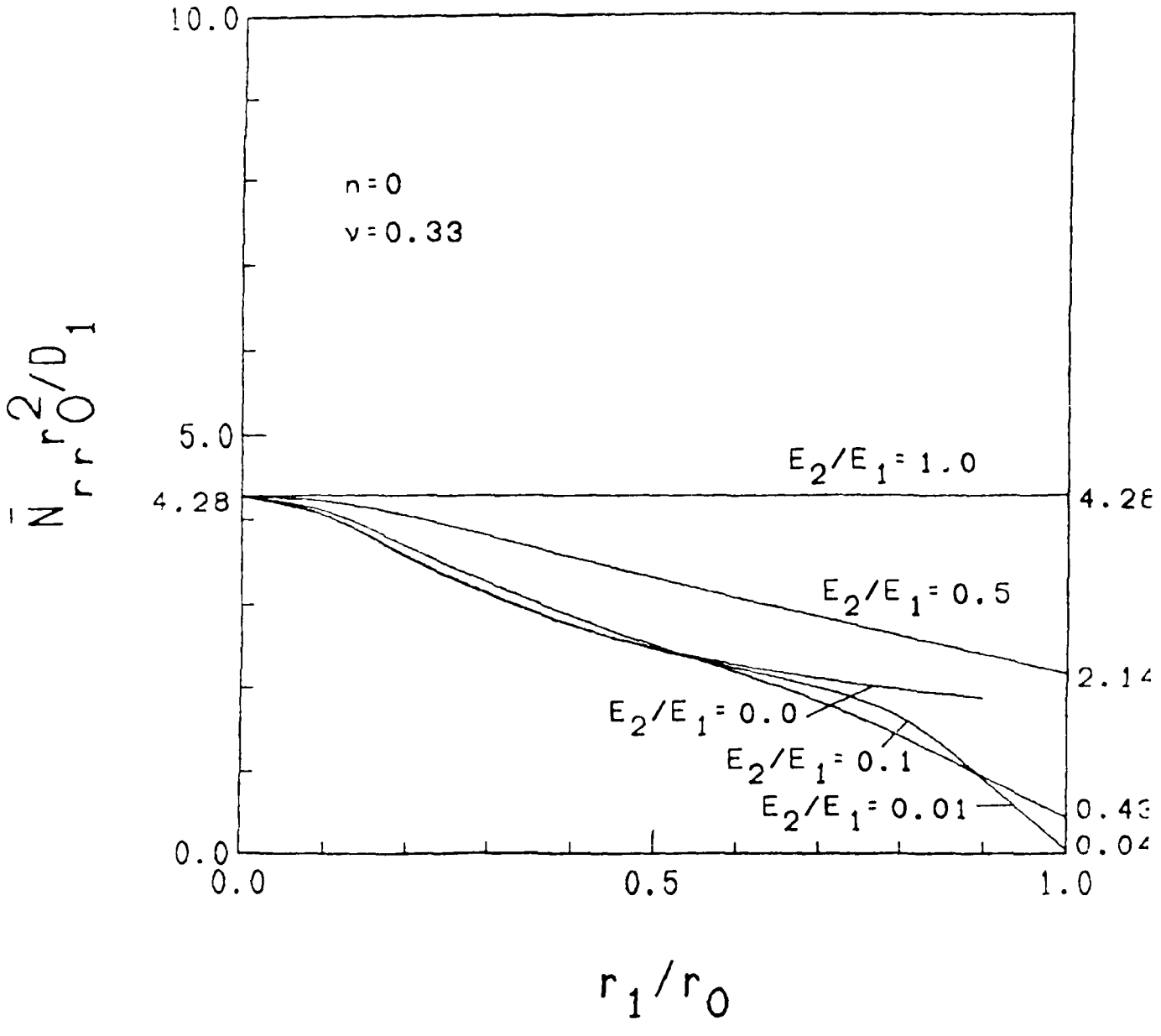

Fig. 4. Critical loads for a two part plate (s.s; n = 0).

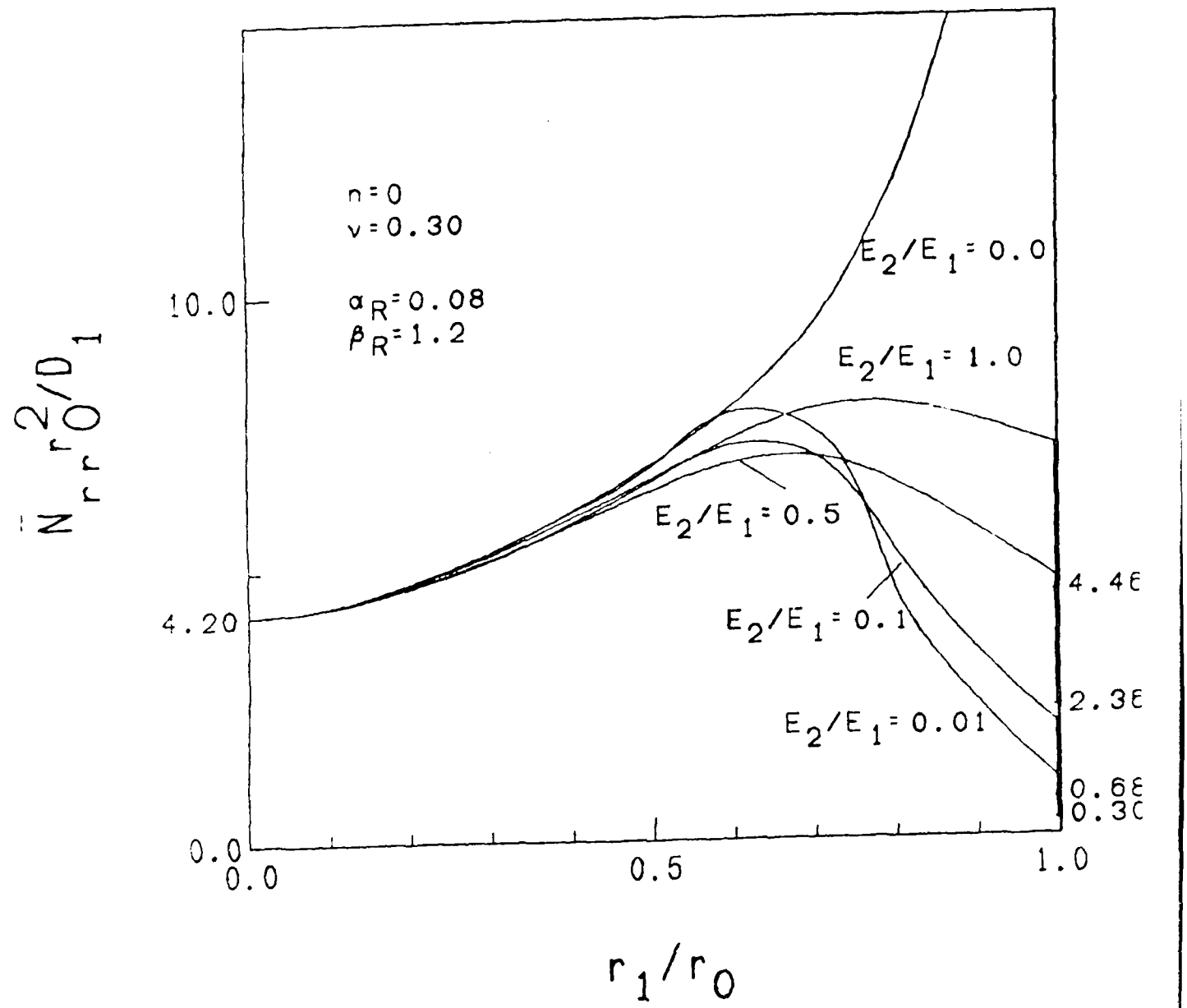

Fig. 5. Critical loads for a ring-stiffened plate (s.s; n = 0).

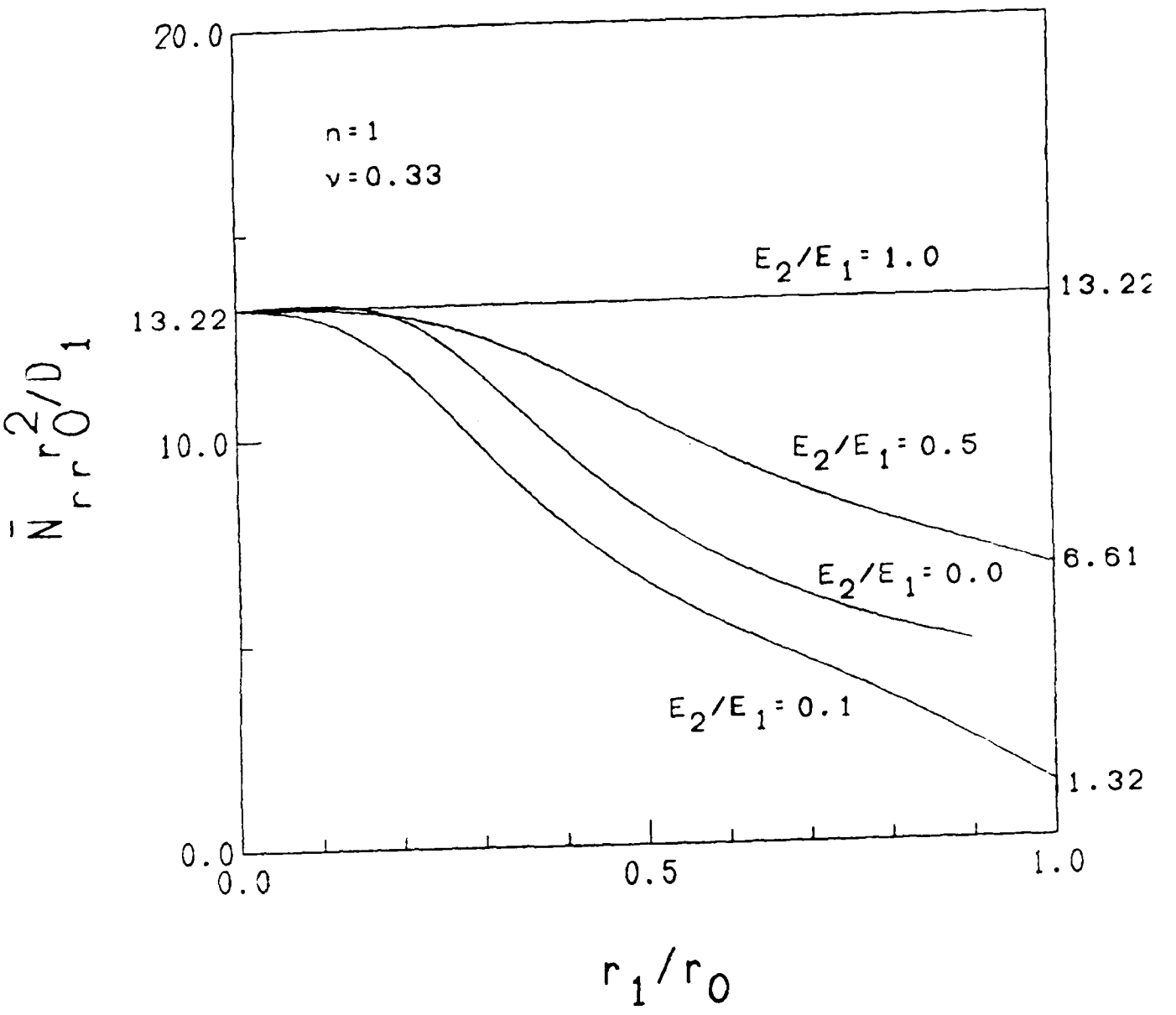

Fig. 6. Critical loads for a two-part plate (s.s; n = 1)

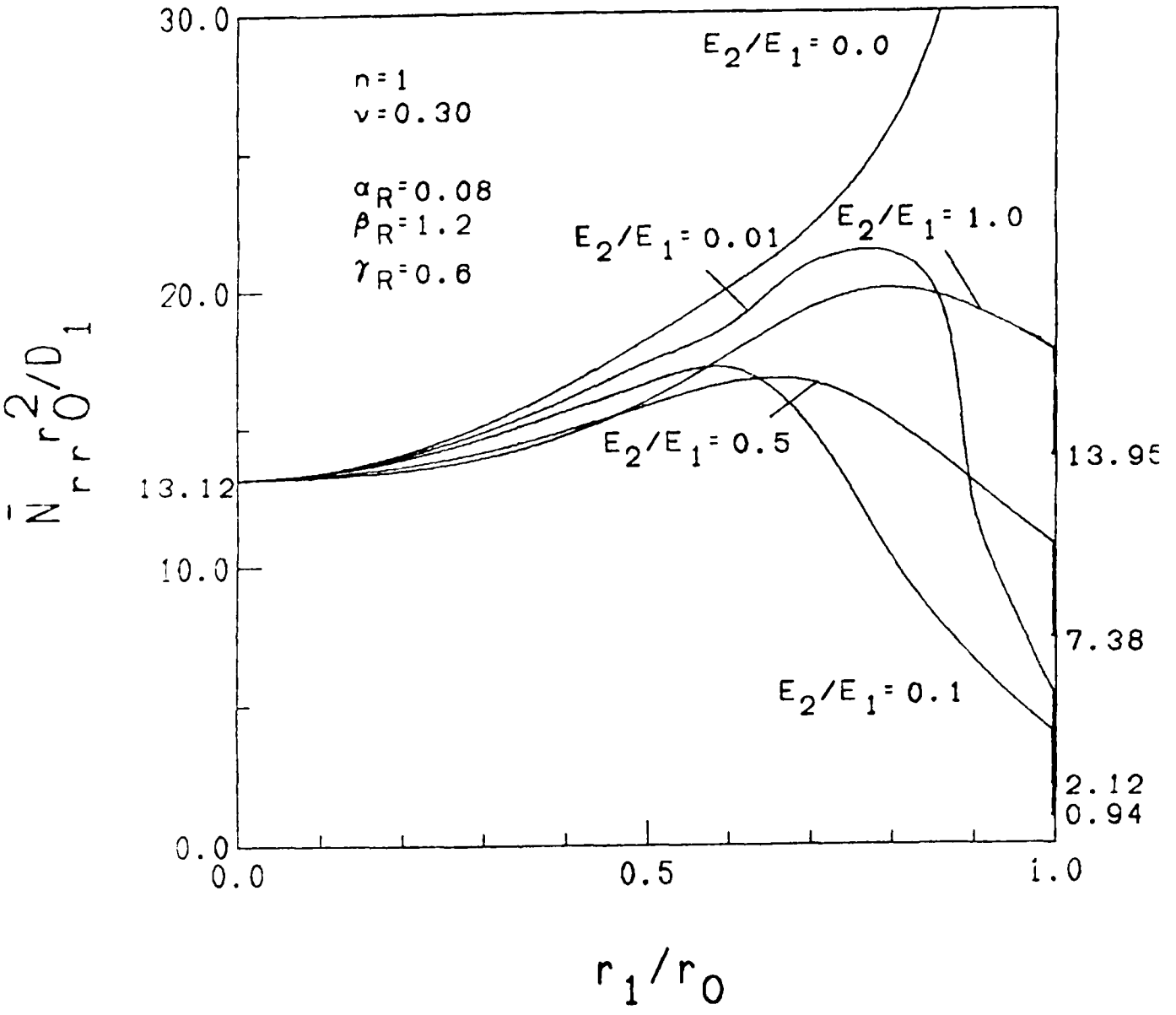

Fig. 7. Critical loads for a ring-stiffened plate (s.s; n = 1)

hand, for r_1/r_o - values larger than 0.55, the critical load is smaller than that of the pure annular plate, and buckling is triggered by the inner and more flexible part. It appears that for $E_2/E_1 = 0.1$, the corresponding curve approaches the value of 0.4282 as r_1/r_o approaches unity (a complete circular plate with bending rigidity equal to one tenth of that of the case $E_2 = E_1$).

(c) In the stiffened case, the central part triggers overall buckling when the stiffener is located between $0.7 < r_1/r_o \leq 1.0$. For values of $r_1/r_o < 0.7$, the modulus of elasticity ratio, E_2/E_1 has small influence, and the critical loads are nearly the same as those corresponding to the stiffened annular plate. For $r_1/r_o \leq 0.7$ (stiffened plate) the decrease in the critical load depends on E_2/E_1. As the inner part becomes more flexible, the "drop" in the critical load becomes much steeper.

(b) For a stiffened plate with an outer edge ring (see figure 5), the buckling load does not converge to the expected value of $4.20\ D_1/r$, but to a higher value. This is so because of the extensional rigidity of the ring, (see equation (7)).

(d) For $0 < E_2/E_1 \leq 1.0$, as the stiffener approaches the plate edge, the restraining effect of the ring is more pronounced and buckling occurs as if the plate (inner part) is partially clamped.

So far, one stiffener geometry ($\alpha_R = 0.08$, $\beta_R = 1.2$ and $\gamma_R = 0.6$) is used, and the study was concentrated on the effect of properties of the two plate parts (E_2/E_1) and the stiffener position, r_1/r_o, for both modes (n = 2 and 1).

Next the effect of stiffener rigidities is studied for two E_2/E_1 values (1.0 and 0.1) for both axisymmetric and asymmetric modes. It is

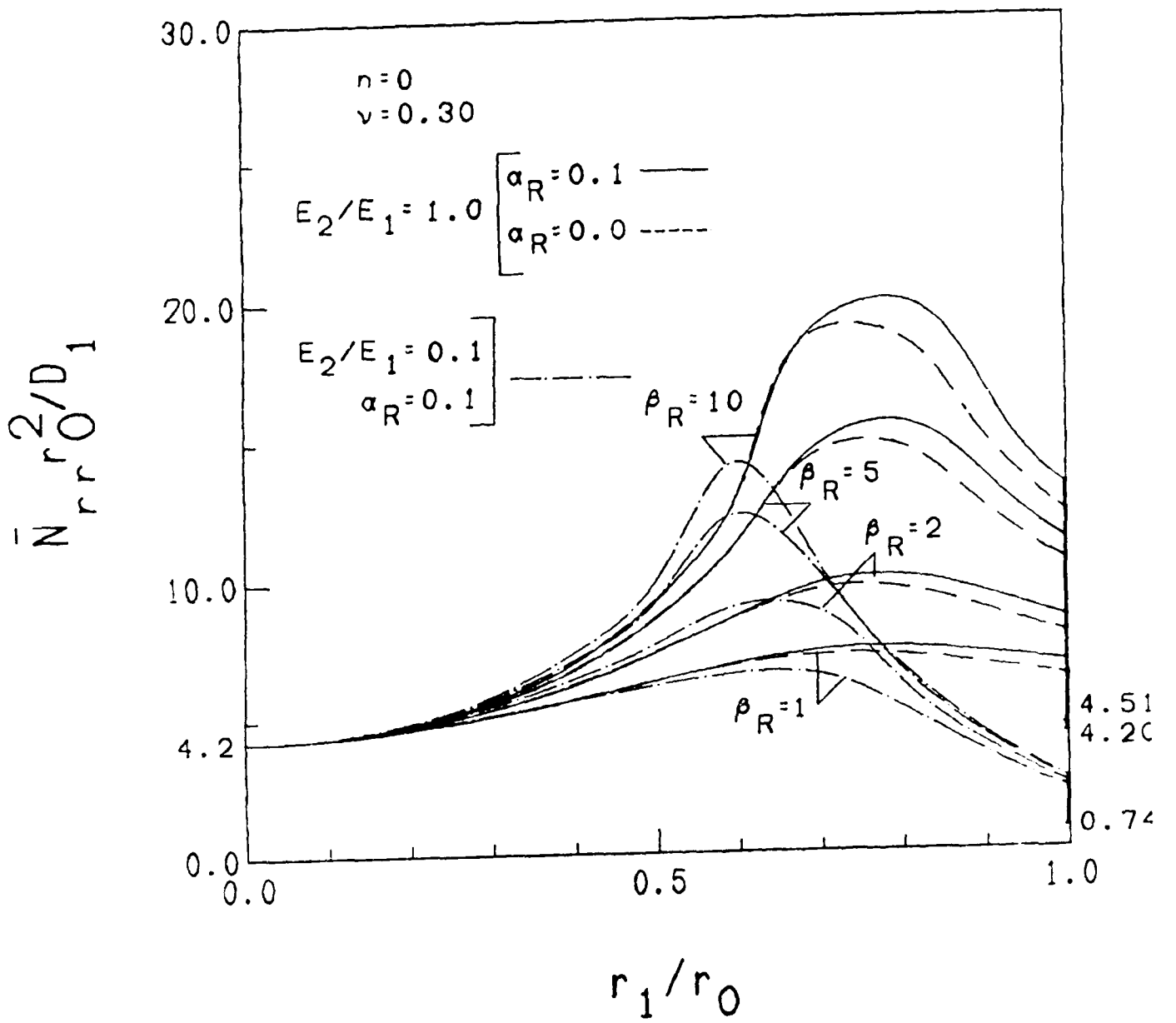

Fig. 5. Effect of flexural stiffness on critical loads (two part stiffened; s.s; n = 0)

done, though, for only one value of α_R (= 0.10). The geometries are governed by:

1) n = 0; α_R = 0.10; ν = 0.3; E_2/E_1 = 1.0, 0.1; and β_R = 1,2,5,10 (axisymmetric)

2) n = 1; α_R = 0.10; ν = 0.3; E_2/E_1 = 1.0, 0.1; β_R = 5; and γ_R = 0.3, 0.5, 0.7, 1.0, 1.5, 2.0.

The results are shown on figures 8 and 9 for n = 0 and n = 1, respectively.

The general trends are similar to those described previously. Moreover, the ring position corresponding to the maximum critical load is smaller for the smaller ratio of the moduli. For E_2/E_1 = 0.1, it is close to r_1/r_o = 0.78. Note that the maxima critical loads are small for the smaller ratio of the moduli, too. Furthermore, the bending stiffness of the ring has a stablizing effect. The higher the stiffness, the higher the critical load. Note that this effect is more pronounced at the higher values of r_1/r_o (r_1/r_o > 0.3). On figure 8, one can also see curves of critical load vs. ring location, r_1/r_o, for E_2/E_1 = 1.0, α_R = 0 and various values of β_R. When these curves are compared to those corresponding to α_R = 0.1, they depict the effect of neglecting the extensional stiffness of the ring (see [10]). Even for this low value of α_R (= 0.10), this effect can be substantial at the higher values of both r_1/r_o and β_R. Finally, when the ring is located at the outer edge, the critical load does not become equal to 4.2 D/r^2 (for E_2/E_1 = 1.0), primarily because of accounting for the axial stiffness of the ring (see equation (7)).

Figure 9 depicts the same results, but for n = 1 (asymmetric mode), α_R = 0.1, β_R = 5.0 and various values of γ_R for both values of the ratio of the moduli, E_2/E_1 = 1.0 and 0.1. Clearly the loads are higher than those

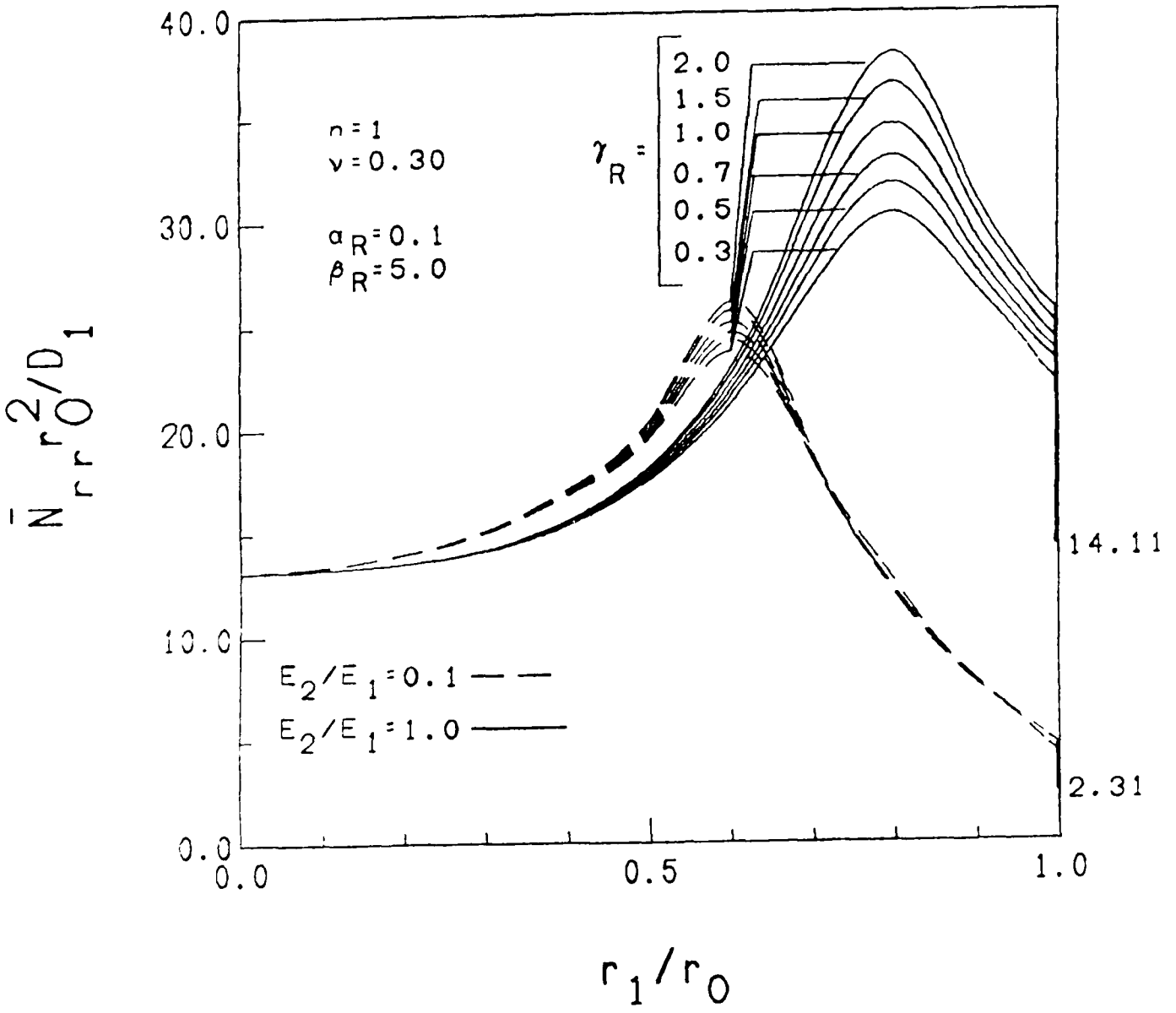

Fig. 9. Effect of Torsional Rigidities (S.S; n = 1)

corresponding to n = 0, therefore, buckling is governed by the axisymmetric mode. Finally, it is shown on figure 9 that the higher the value of the rotational stiffness parameter, γ_R, the higher the critical load (for n = 1), as expected.

Clamped Multi-Annular Plates

Another example consists of a multi-annular plate clamped and loaded at the outer edge. The load is radial and axisymmetric. The parameters considered in this case are:

ν = 0.3; E_2/E_1 = 0, 0.1, 0.5, and 1.0;

for n = 2 α_R = 0.08 and β_R = 1.2; and

for n = 1, α_R = 0.08 and β_R = 1.2 and γ_R = 0.6

The trends which are observed in the simply supported case are mostly the same here. The results are presented for the unstiffened plate on figure 10, and on figures 11 and 12 for the stiffened plate.

A comparison between the unstiffened case and the stiffened one shows that that the stiffener increases the buckling capacity of the plate. Regardless of the presence of stiffening, when the ratio of the moduli is small, E_2/E_1, buckling is triggered by the central part and the critical load is decreasing as the common boundary approaches the outer edge.

Note that on figure 11, results corresponding to the annular plate, E_2/E_1 = 0, are only shown for $r_1/r_o < 0.55$. It has been shown [11] that for $r_1/r_o > 0.55$ higher (n > 0) buckling modes govern and thus the critical load corresponds to higher values of n.

The presence of stiffening, figures 11 and 12, shows critical loads for stiffened annular plates (E_2/E_1 = 0). From figure 12, one observes that buckling is governed by the axisymmetric mode. This is true for the range of results $r_1/r_o < 0.7$.

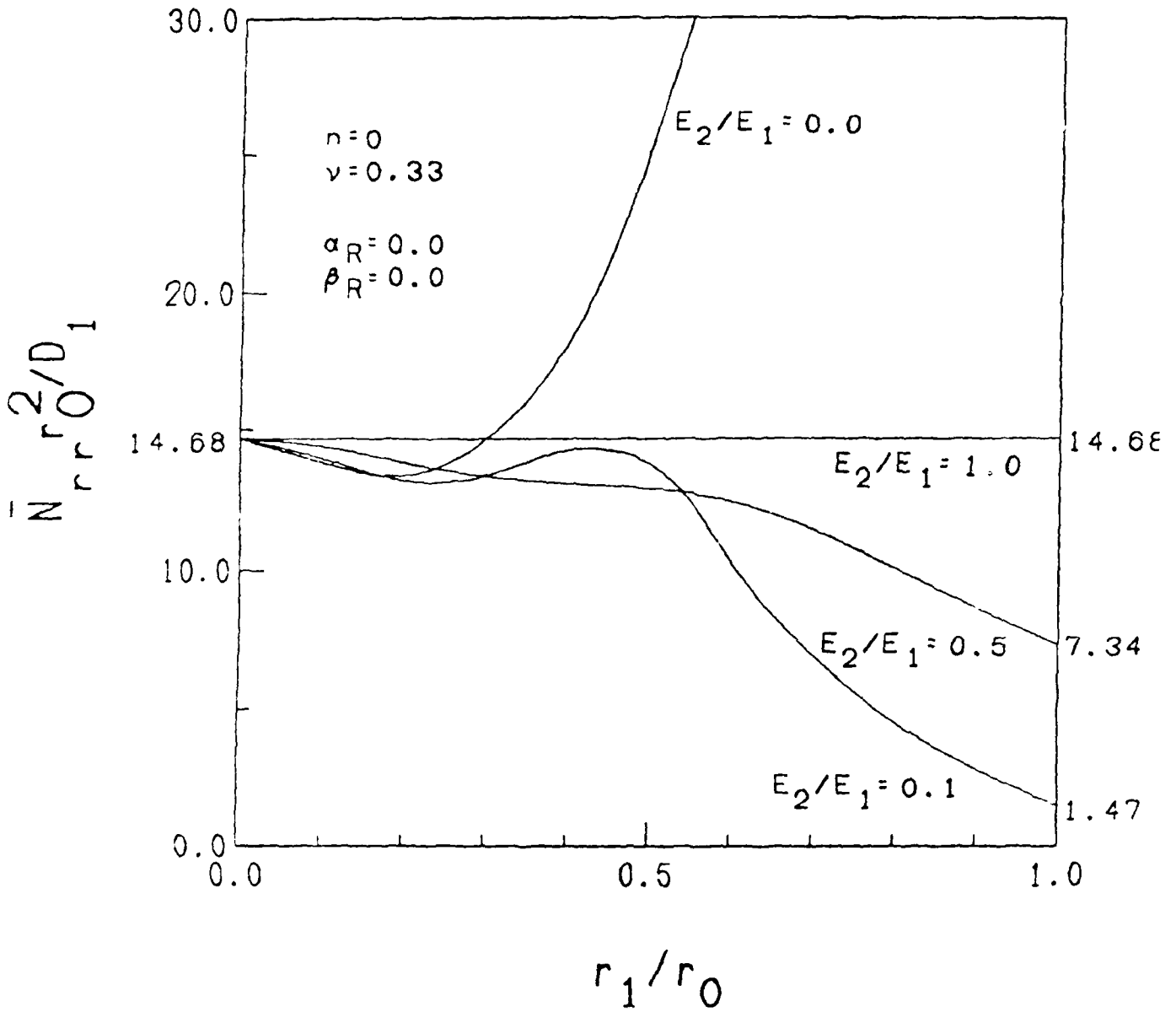

Fig. 10. Critical loads for a two-part plate (clamped; n = 0)

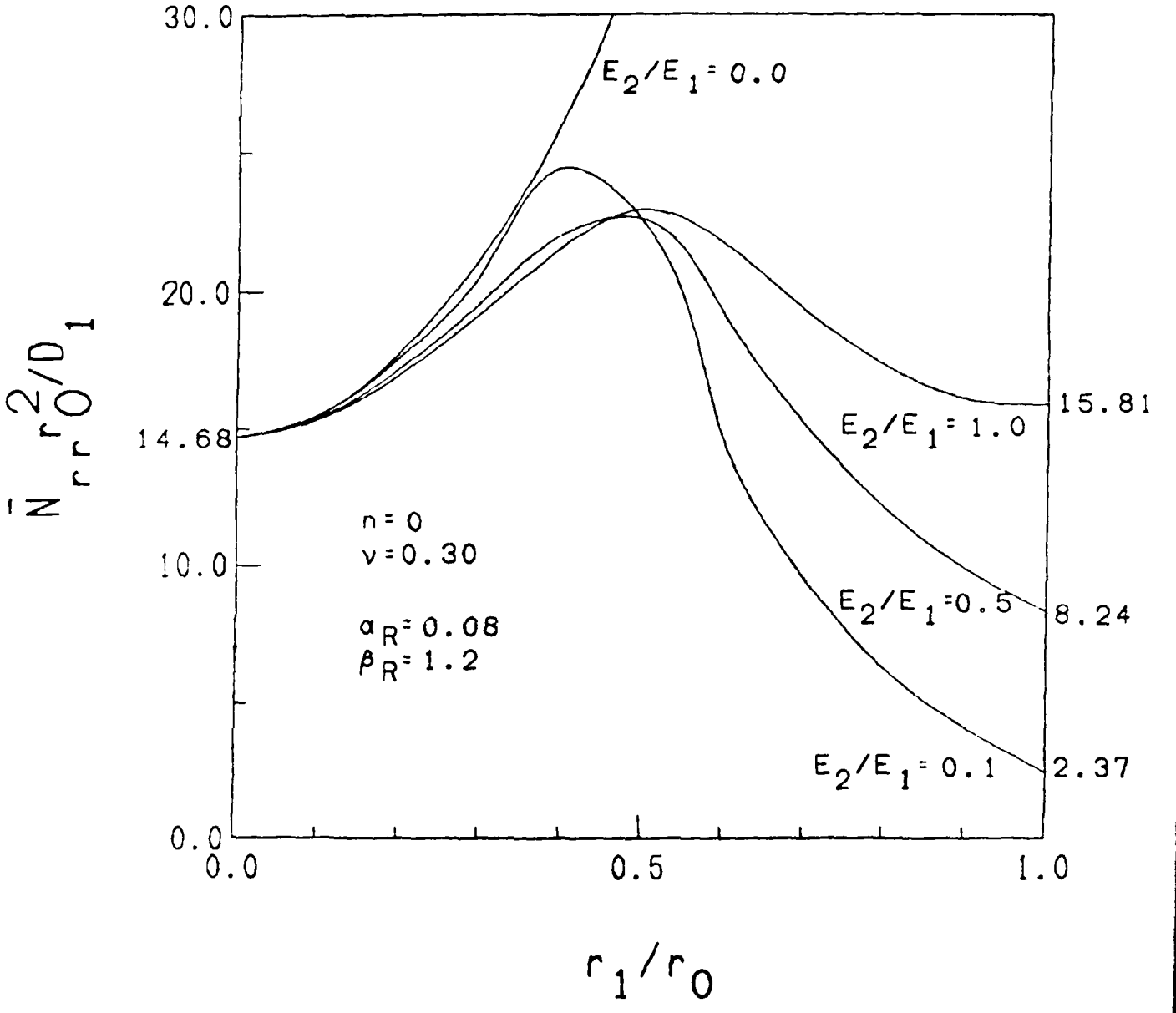

Fig. 11. Critical loads for a ring-stiffened plate (clamped; n = 0)

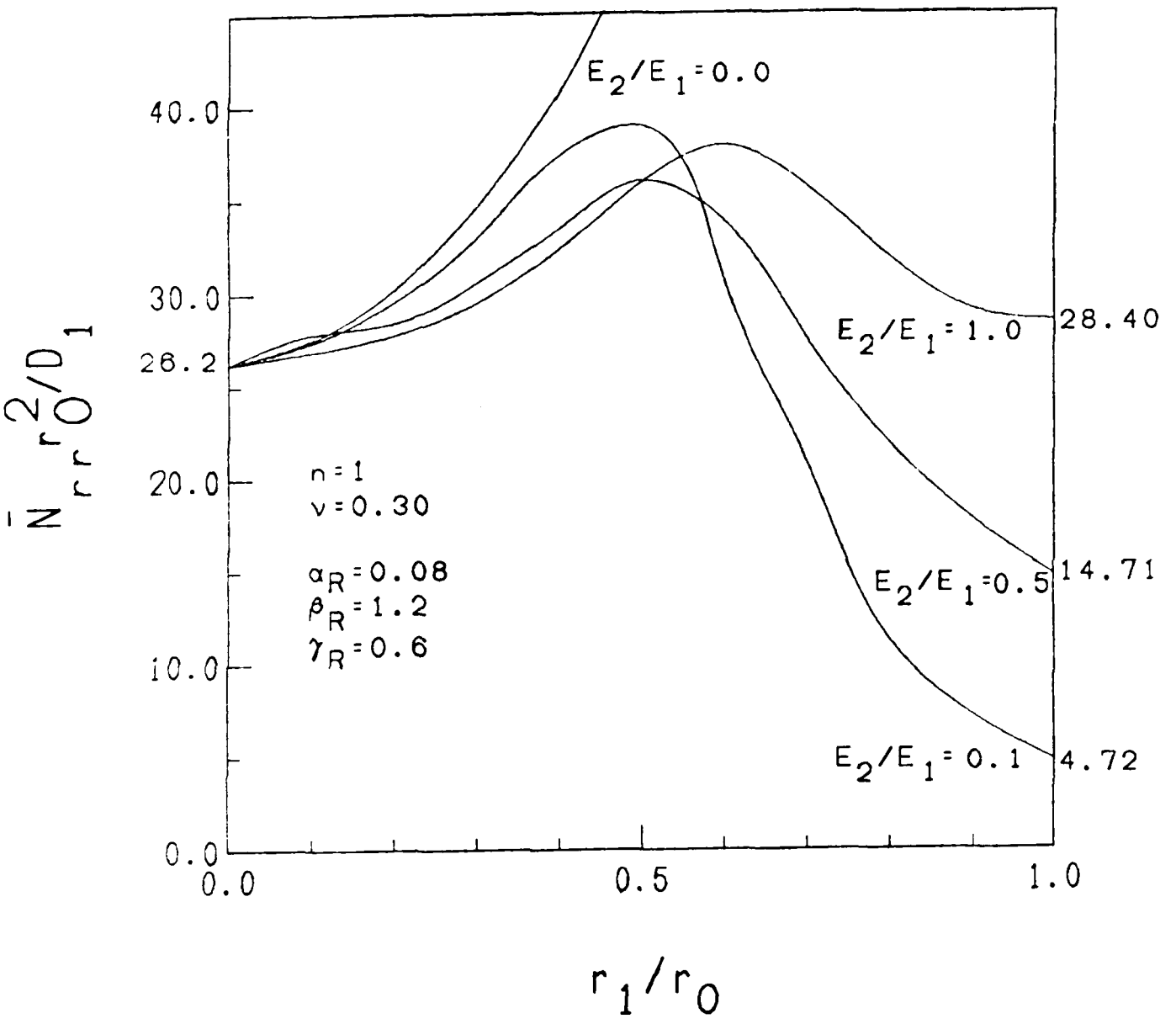

Fig. 12. Critical loads for a ring-stiffened plate (clamped; n = 1)

For flexible inner plates, $E_2/E_1 \neq 0$, but with $0 < E_2/E_1 \leq 1.0$, and a stiffener at the common joint, buckling is governed by the axisymmetric mode.

Analysis of a Ring-stiffened Plate Using Plate Theory.

In this section a different approach is used for the analysis of a homogeneous circular plate stiffened by a ring somewhere between the center and the edge. The stiffener, in this case, is modelled by a very narrow annular plate, with different geometrical and material properties. The analysis carried out is that of a three-part plate, where the outer and central parts have the same properties, and the middle part represents the stiffener.

This type of analysis is correct, provided that plate theory assumptions hold true for the ring part, as well. The ring plate geometry and properties were adjusted in order to yield the following values for ring type of stiffnesses. (This was done in order to be able to compare the present results with those using ring stiffeners).

$\alpha_R = 0.1$ with $\beta_R = 10$

for n = 0

$\alpha_R = 0.2$ with $\gamma_R = 20$

$\alpha_R = 0.1$ with $\beta_R = 1.0$, $\gamma_R = 0.35$ for n = 1.

The results are shown graphically on figure 13 for n = 0 (axisymmetric) and figure 14 for n = 1.

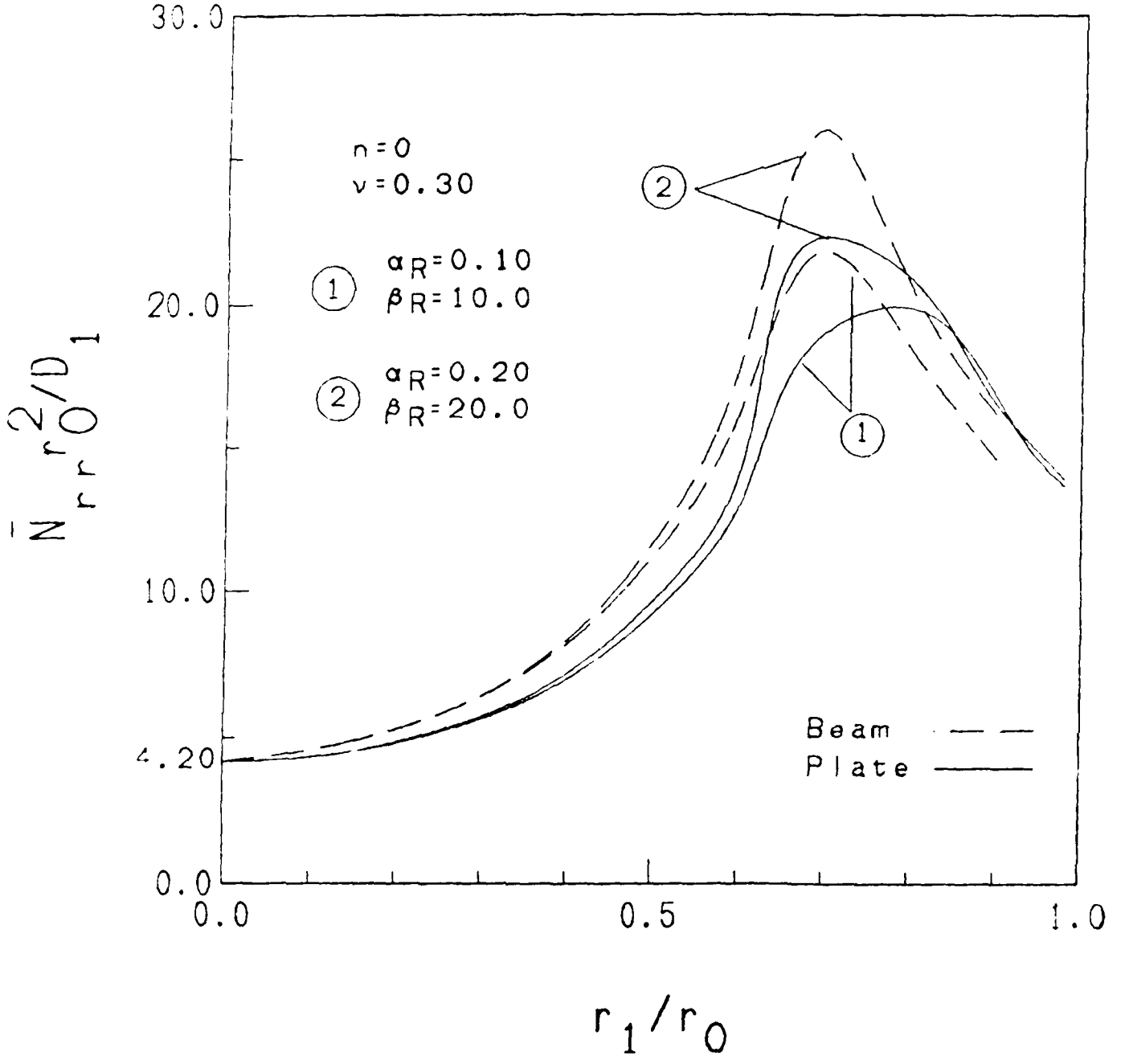

Fig. 13. Critical loads by two different approaches (s.s; n = 0)

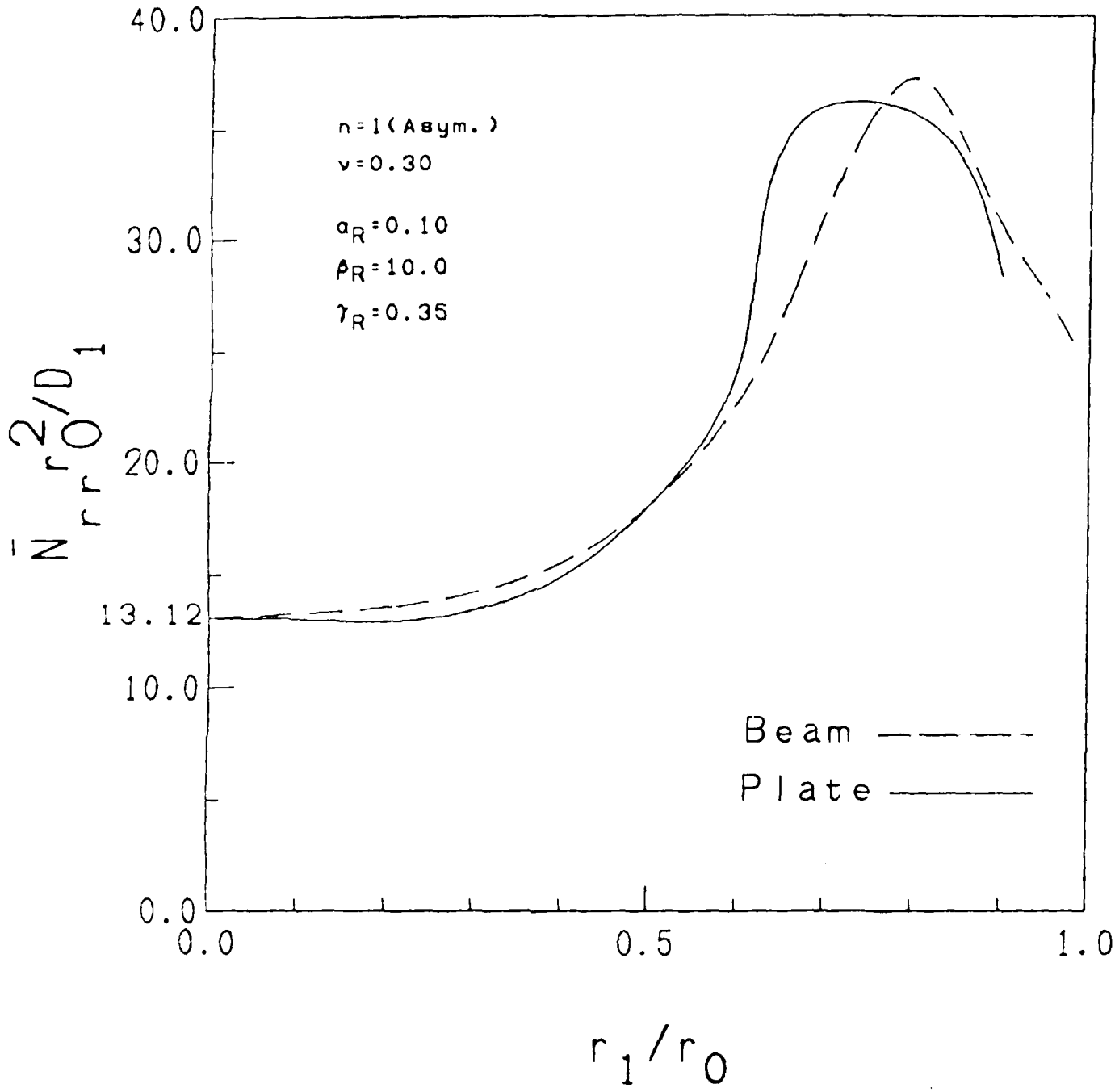

Fig. 14. Critical loads by two different approaches (S.S; n = 1)

It is seen from these figures that, the comparison is fairly good. One must realize that in one case the stiffener is considered as a curved beam and in the other as an annular plate.

CONCLUSIONS

Among the many conclusions of the parametric studies one may list the following important ones:

1) Stiffening, regardless of boundary conditions at the outer loaded edge, has a stabilizing effect. The higher the bending stiffness of the ring, the higher the critical load. Moreover the extensional ring stiffness improves the critical load. The effect of bending stiffness is [illegible] for ring locations higher than $0.3\ r_o$. Similarly, the effect of extensional ring stiffness becomes important for ring locations higher than $0.7 r_o$. These conclusions are true for simply-supported boundaries, but the trends are also true for clamped boundaries.

2) Modelling the stiffener as an annular plate yields critical loads, which are close to those corresponding to modelling the ring as a curved beam. Note that the latter modelling is more general, because it can accommodate various ring geometries instead of only rectangular cross section rings.

3) The use of a single ring, for stiffening a circular plate, implies also an optimum position. For a homogeneous plate, the optimum position corresponds to approximately $r_1/r_o = 0.7$ for simply supported boundaries and $r_1/r_o = 0.5$ for clamped ones. These optimal locations change when the two parts of the plate have different properties.

ACKNOWLEDGEMENTS

This work was supported by the United States Air Force Office of Scientific Research, under Grant Number AFOSR 83-0243. This financial support is gratefully acknowledged.

REFERENCES

1. Dean, W. R., "The Elastic Stability of an Annular Plate," Proceedings of the Royal Society of London, England, Ser. A., Vol. 106, 1924, pp. 268-284.

2. Federhofer, K. and Egger, H., "Knickung der auf Scherung beanspruchten Kreisringplatte mit veranderlicher Dicke," Ingenieur-Archiv, Vol. 14, 1943, pp. 155-166.

3. Yamaki, N., "Buckling of Thin Annular Plate under Uniform Compression," Journal of Applied Mechanics, June 1958, pp. 267-273.

4. Mansfield, E. H. "On the Buckling of Annular Plates", Quarterly J. of Mechanics and Applied Mechanics" , Vol. 13, No. 1, Feb., 1960, pp. 16-23.

5. Bareeva, N. and Lizarev, S. D., "Nonaxisymmetric Modes of Stability Loss in Annular Plates in Nonuniform Stress Field", Insh. Zh. Mech. Tverd, Tele., Vol. 5, No. 3, 1965, pp. 103-105.

6. Lizarev, S. D. and Bareeva, G. N., "Stability of an Elastically-Fastened Annular Plate in a Nonuniform Stress Field," Insh. Zh. Mech. Tverd, Tele., Vol. 5, No. 3, 1965, pp. 483-491.

7. Lizarev, S. D., "Stability of Annular Plates in a Non-Uniform Stress Field", (Translation), Prikladnaya Mekhanika, Vol. 16, No. 6, 19[illegible], pp. 92-97.

8. Majumdar, S., "Buckling of a Thin Annular Plate [illegible] Compression," AIAA Journal, No. 9, 1971, pp. 1701-17[illegible].

9. Dimitsos, G. J. and Blackmon, J. M., "Buckling [illegible] Stiffened, Thin Circular Plates", AIAA J., Vol. [illegible], [illegible], pp. 1205-1208.

10. [illegible]bottom, J. N., and Miller, N. E., "[illegible] Ring-Stiffened Circular Plates", J. Appl. M[illegible], Vol. [illegible], No. [illegible], pp. 654-[illegible].

[9] Simitses, G. J., Sallam, S., Frostig, Y., "Buckling of Delaminated Shells and Multi-Annular Plates", Interim Scientific Report to AFOSR; AFOSRTR-XXXX, School of Engineering Science and Mechanics, Georgia Institute of Technology, Atlanta, GA., October 1985.

[10] Frostig, Y., and Simitses, G. J., "Buckling of Ring Stiffened Multi-Annular Plates" submitted for publication to Computers and Structures.

BUCKLING OF LAMINATED CIRCULAR PLATES

Yeoshua Frostig* and George J. Simitses**
School of Engineering Science and Mechanics
Georgia Institute of Technology, Atlanta, Georgia

ABSTRACT

The manuscript deals with buckling of complete and annular circular plates, made of symmetric laminates with general orientation of the lamina fibers. The plate is subjected to an in-plane, symmetric, destabilizing load. The load is applied at the outer edge for the complete plate and at the outer and inner edges for the annular one. The plate is supported in various ways along its boundaries.

The paper includes the derivation of the governing equations and discusses the various methods of solution. Numerical results are presented for a clamped plate.

Introduction

Fiber reinforced laminated composites are fastly and widely replacing metals as construciton materials, especially in the manufacture of surface, air and space vehicles. Thin plates and shells are popular structural elements. Such configurations, in service, are mostly and often subjected to external loads which may induce buckling. In many situations buckling is an undesirable phenomenon and it forms a primary consideration for design. Because of this, stability of laminated plates and shells continues to attract the attention of the structural engineer.

Most of the analyses reported in the open literature [1-5] for circular configurations are limited to polar orthotropy, a case for which the various rigidities are constant with respect to the radial and circumferential coordinates. Another group of plates employs rectilinear orthotropy for which results are reported in the open literature [6-7]. The analysis, for this group is limited to vibration problems only. The buckling of laminated composite plates is usually limited to rectangular plates [8-9]. A very detailed survey based on hundreds of references by Leissa [10], on composite plates, discusses results and analyses for only rectangular configurations.

The manuscript includes the derivation of the governing equations and discusses the various methods of solutions. The analysis deals with buckling of circular laminated composite plates, loaded by in-plane axisymmetric forces at the edges. The geometry is limited to symmetric regular angle ply configurations and lamination theory [8,11] is employed. The solution proposed in the paper is based on the Galerkin and the modified Galerkin procedures. The plates considered herein are either clamped or simply supported.

Mathematical Formulation

The geometry consists of a circular laminated plate subjected to axisymmetric loading at the edges (see Fig. 1). The laminate is a symmetric, regular, angle-ply one [8].

The governing equations for the primary state are [11]:

$$(rN^o_{rr})_{,r} + N^o_{r\theta,\theta} - N^o_{\theta\theta} = 0$$

$$N^o_{\theta\theta,\theta} + (rN^o_{r\theta})_{,r} + N^o_{r\theta} = 0 \qquad (1)$$

Moreover, the buckling equation, in terms of moments and force resultants, after neglecting the small non-linear terms, is (see Appendix B).

$$(rM_{rr})_{,rr} + 2\,(M_{r\theta,r\theta} + \frac{1}{r} M_{r\theta,\theta}) + (\frac{1}{r} M_{\theta\theta,\theta\theta} + -M_{\theta\theta,r}) + r\,[N^o_{rr} w_{,rr} + N^o_{\theta\theta} (\frac{w_{,\theta\theta}}{r^2} + \frac{w_{,r}}{r}) + 2N^o_{r\theta} (\frac{w_{,r\theta}}{r} - \frac{1}{r^2} w_{,\theta})] = 0 \qquad (2)$$

where N^o_{rr}, $N^o_{\theta\theta}$, $N^o_{r\theta}$ are the primary state stress resultants, M_{rr}, $M_{\theta\theta}$, $M_{r\theta}$ are the bending and twisting moment resultants; w the transverse displacement, and r,θ the coordinates in the radial and circumferential directions, respectively.

The in-plane, primary state, kinematic relations are given by

$$\varepsilon^o_{rr} = u_{,r}$$

$$\varepsilon^o_{\theta\theta} = v_{,\theta}/r + u/r \qquad (3)$$

$$\gamma^o_{r\theta} = v_{,r} + u_{,\theta}/r - v/r$$

where u,v are the deformations in radial and circumferential directions, respectively. Note that the transverse displacement (w^o) is zero in the primary state. The relations between the stress resultants and the in-plane (reference plane) strains are

*Postdoctoral Fellow; on leave from Technion-Israel Institute of Technology, Haifa, Israel.
**Professor, Associate Fellow of AIAA; Member ASME

$$\begin{Bmatrix} N^{o}_{rr} \\ N^{o}_{\theta\theta} \\ N^{o}_{r\theta} \end{Bmatrix} = \begin{bmatrix} A_{11} & A_{12} & A_{14} \\ A_{12} & A_{22} & A_{24} \\ A_{14} & A_{24} & A_{44} \end{bmatrix} \begin{Bmatrix} \epsilon^{o}_{rr} \\ \epsilon^{o}_{\theta\theta} \\ \gamma^{o}_{r\theta} \end{Bmatrix} \qquad (4)$$

where $A_{ij} = \sum_{k=1}^{N} \int_{h_{k-1}}^{h_k} \bar{Q}^{(k)}_{ij} dz$, and the $\bar{Q}^{(k)}_{ij}$ are defined in Appendix A.

The terms A_{ij} are θ-dependent and they also depend on the relative fiber orientation between the various layers.

Two formulations can be used for the primary state analysis. Note that in order to solve the buckling equation we need the primary state stress resultants, N^{o}_{rr}, $N^{o}_{\theta\theta}$ and $N^{o}_{r\theta}$ in terms of the applied loadings. If some of the in-plane boundary conditions are kinematic then the kinematic approach is used for solving the primary state. On the other hand, if the in-plane boundary conditions are natural then the force approach is employed. For details see Appendix B.

The kinematic formulation in terms of u and v is straightforward. The governing equations are derived by substitution of Eqs. (3) and (4) into Eq. (1) yielding:

$$[r(A_{11}u_{,r} + A_{12}v_{,\theta} + A_{14}(u_{,\theta} + v_{,r}))]_{,r}$$

$$- (A_{11}u_{,r} + A_{22}v_{,\theta} + A_{24}(u_{,\theta} + v_{,r})) +$$

$$+ (A_{14}u_{,r} + A_{24}v_{,\theta} + A_{44}(u_{,\theta} + v_{,r}))_{,\theta} = 0 \qquad (5)$$

$$[A_{12}u_{,r} + A_{22}v_{,\theta} + A_{24}(u_{,\theta} + v_{,r})]_{,\theta} +$$

$$+ [r(A_{14}u_{,r} + A_{24}v_{,\theta} + A_{44}(u_{,\theta} + v_{,r}))]_{,r}$$

$$+ A_{14}u_{,r} + A_{24}v_{,\theta} + A_{44}(u_{,\theta} + v_{,r}) = 0 \qquad (6)$$

Since the A_{ij} coefficients are θ-dependent, the derivatives with respect to θ are not null and must be included in the equations.

The force approach determines the stress distribution by the introduction of the Airy stress function through the in-plane compatibility equation. The Airy stress function and primary stress resultants are given by [12].

$$N^{o}_{rr} = F_{,r}/r + F_{,\theta\theta}/r^2$$

$$N^{o}_{\theta\theta} = F_{,rr} \qquad (7)$$

$$N^{o}_{r\theta} = -(F_{,\theta}/r)_{,r}$$

and the compatibility equation is:

$$\epsilon^{o}_{rr,\theta\theta} - r\epsilon^{o}_{rr,r} + r(r\epsilon^{o}_{\theta\theta})_{,rr} - (r\gamma^{o}_{r\theta})_{,r\theta} = 0 \qquad (8)$$

Substitution of Eqs. (7) into Eq. (8) and use of Eqs. (4) yield

$$a_{22}r^4F_{,rrrr} + (2a_{22} - a_{24,\theta})r^3F_{,rrr} - 2a_{24}r^3F_{,rrr\theta}$$

$$+ (-2a_{24,\theta} + a_{12,\theta\theta} - a_{11} - a_{14,\theta})r^2F_{,rr} +$$

$$+ (2a_{12} + a_{44})r^2F_{,rr\theta\theta} + (2a_{12} + a_{44,\theta})r^2F_{,rr\theta} +$$

$$(a_{11} + a_{11,\theta\theta} - a_{14,\theta})rF_{,r} + (-a_{14,\theta\theta} - 2a_{14} +$$

$$+ 2a_{11,\theta} - 2a_{24})rF_{,r\theta} - 2a_{14}rF_{,r\theta\theta} +$$

$$(a_{14,\theta\theta} + 2a_{14} + 2a_{24})F_{,\theta} + (a_{11,\theta\theta} + a_{44} + 2a_{14,\theta}$$

$$+ 2a_{11} + 2a_{12})F_{,\theta\theta} + (2a_{14} + 2a_{11,\theta})F_{,\theta\theta\theta} +$$

$$+ a_{11}F_{,\theta\theta\theta\theta} = L_F F = 0 \qquad (9)$$

where $[a_{ij}] = [A_{ij}]^{-1}$ and L_F is the differential operator of the equation.

The coefficients in the above equation are in general θ-dependent. There is no closed form solution and an approximate one can be derived through the Galerkin procedure by assuming

$$F(r,\theta) = F_o(r,\theta) + \sum_{n=1}^{\infty} a_n F_n(r,\theta) \qquad (10)$$

where $F_o(r,\theta)$ is chosen in such a way that it satisfies the boundary conditions. Thus, the stresses due to function $F_n(r,\theta)$ must vanish at the boundaries. The unknown coefficients, a_n, are evaluated through the Galerkin integrals, or

$$\int_A [L_F(F(r,\theta))] F_m dA = 0 \qquad (m = 1,\ldots,\infty) \qquad (11)$$

The functions $F_n(r,\theta)$ must satisfy the following boundary conditions;

$$N^{o}_{rr} = 0 = F_{n,r}/r + F_{n,\theta\theta}/r^2$$

$$N^{o}_{r\theta} = 0 = -F_{n,r\theta}/r + F_{n,\theta}/r^2 \qquad \text{at } r = R_1 \qquad (12)$$

If $F_n(r,\theta) = f_n(r)\cos n\theta$ then the above conditions can be replaced by:

$$f_n(r) = 0$$

$$f_{n,r}(r) = 0 \qquad \text{at } r = R_1 \qquad (13)$$

Namely, the functions $f_n(r)$ can be chosen to be the deflection functions of a clamped plate.

In the case of a circular plate, loaded at the outer edge the functions are:

$$f_n(r) = r^{n-1}(r-R_o)^2 \qquad (n = 1...\infty) \qquad (14)$$

where R_o is the outer radius.

In the case of an annular plate, loaded at the inner and at the outer edges, the functions considered are:

$$f_n(r) = (r - R_o)^2(r - R_1)^{n+1} + (r-R_1)^2(r-R_o)^{n+1}$$

$$(n = 1 ...\infty) \qquad (15)$$

where R_o and R_1 are the outer and inner radii, respectively.

In the case of a circular plate, loaded axisymmetrically at the edge, or an annular plate loaded at the outer and inner edges with the same intensity, an analytical closed form solution exists, provided that the plate has cylindrical orthotropy. The function is given by $F = Cr^2$, where C is determined through the force boundary conditions. In the case of a laminated plate, with $(+30^o/-30^o)_{ns}$, this solution is acceptable within some engineering accuracy. The error in the compatibility equation, Eq. (9) is of the order 10^{-4}, instead of zero. In general, the solution procedure proposed earlier should be followed.

The buckling equation, in terms of the transverse displacement, is derived by using the following kinematic relations [11]:

$$\chi_{rr} = -w_{,rr}$$

$$\chi_{\theta\theta} = -w_{,\theta\theta}/r^2 - w_{,r}/r \qquad (16)$$

$$\chi_{r\theta} = -(-w_{,r\theta}/r + w_{,\theta}/r^2)$$

where χ_{rr}, $\chi_{\theta\theta}$, $\chi_{r\theta}$ are the radial, circumferential and torsional curvature changes of the plate midsurface. The moment-strain relations are derived through integration through the thickness and are given by (Note that there is no coupling between bending and stretching)

$$\begin{Bmatrix} M_{rr} \\ M_{\theta\theta} \\ M_{r\theta} \end{Bmatrix} = \begin{bmatrix} D_{11} & D_{12} & D_{14} \\ D_{12} & D_{22} & D_{24} \\ D_{14} & D_{24} & D_{44} \end{bmatrix} \begin{Bmatrix} \chi_{rr} \\ \chi_{\theta\theta} \\ \chi_{r\theta} \end{Bmatrix} \qquad (17)$$

where $D_{ij} = \sum_{k=1}^{h} \int_{h_{k-1}}^{k} \bar{Q}_{ij}^{(k)} z^2 dz$

Substitution of Eqs. (14) and (16) into Eq. (2) yields:

$$-w_{,rrrr}(D_{11}) + w_{,rrr}(2D_{11} + 2D_{14,\theta}) + w_{,rrr\theta}(4D_{14})$$

$$+ w_{,rr}(2D_{24,\theta} + 2D_{14,\theta} - D_{22} + D_{12,\theta\theta}) / r +$$

$$w_{,rr\theta}(4D_{44,\theta} + 2D_{12,\theta}) / r +$$

$$w_{,rr\theta\theta}(2D_{12} + 4D_{44})/r + w_{,r}(D_{22} + D_{22,\theta\theta}) / r^2 +$$

$$w_{,r\theta}(4D_{14} - 4D_{44,\theta} + 2D_{24,\theta\theta} + 2D_{22,\theta\theta} + 4D_{24})/ r^2 +$$

$$w_{,r\theta\theta}(-2D_{12} - 4D_{44} + 6D_{24,\theta}) / r^2 +$$

$$w_{,r\theta\theta\theta}(4D_{24})/r2 + w_{,\theta}(-4D_{14} + 4D_{44,\theta} + 4D_{24} +$$

$$- 2D_{24,\theta\theta}) /r^3 + w_{,\theta\theta}(2D_{12} + 2D_{22} - 6D_{24,\theta} + 4D_{44} +$$

$$+ D_{22,\theta\theta}) / r^3 +$$

$$w_{,\theta\theta\theta}(-4D_{24} + 2D_{22,\theta})/r^3 + w_{,\theta\theta\theta\theta}(D_{22}) / r^3 +$$

$$r\left[N^o_{rr}w_{,rr} + N^o_{\theta\theta}(w_{,\theta\theta}/r^2 + w_{,r}/r) + \right.$$

$$\left. + 2N^o_{r\theta}(w_{,r\theta}/r - w_{,\theta}/r^2)\right] = 0 \qquad (18)$$

where N^o_{rr}, $N^o_{\theta\theta}$ and $N^o_{r\theta}$ are the radial, circumferential and shear primary stress resultants. The coefficients in the above equation, Eq. (18), are θ-dependent and the partial derivatives with respect to θ must be considered.

The solution in general, even for the simplest of cases, is very complicated. An approximate solution approach, based on the Galerkin procedure, is employed. It is outlined, with sufficient detail, in the next section.

Solution of the Buckling Equation

Two variations of the Galerkin procedure are employed, herein, in order to achieve a solution for the buckling equation.

The first one is the strict Galerkin procedure, which employs a series solution (approximation) such that each term in the series satisfies all boundary conditions, regardless of their nature (kinematic and/or natural). The second one is the modified Galerkin procedure [13]. In this case, each term of the series need only satisfy the kinematic boundary conditions. Then minimization of the error includes boundary terms along with the Galerkin integrals.

The approximate solution is equal to (truncated series):

$$w_a(r,\theta) = \sum_{n=0}^{N} A_n w_n(r) \cos n\theta \qquad (19)$$

where: $w_n(r)$ are functions of r; A_n undetermined constant and n denotes the number of terms. The assumed function to be used with the regular Galerkin procedure [13], must satisfy all boundary conditions at the various edges of the plate. The radial function coefficients are determined in such a way that all the boundary conditions are satisfied.

In order to clarify this, let us consider the following two cases for a complete circular plate.

Case a. A clamped plate at $r = R_o$.

The boundary conditions for this case are:

$$w_n(R_o,\theta) = 0 \qquad ; \qquad w_{,r}(R_o,\theta) = 0 \tag{20}$$

Thus, substitution of the assumed solution, Eq. (19) into these boundary conditions yields:

$$w_n(R_o) = w_{n,r}(R_o) = 0 \tag{21}$$

A_n is determined through the application of the Galerkin procedure on the buckling equation, Eq. (18).

Case b. A simply supported circular plate. The boundary conditions for this plate are given by:

$$w_n(R_o,\theta) = 0$$

$$M_{rr}(R_o,\theta) = 0 = \left[-D_{11} w_{,rr} - D_{12} (w_{,\theta\theta}/r^2 + w_{,r}/r) \right.$$

$$\left. 2(D_{12} w_{,rr}/r + w_{,\theta}/r^2)) \right|_{r = R_o} \tag{22}$$

Substitution of the assumed solution Eq. (19), into Eq. (22) after some algebraic manipulations yields the following equivalent boundary conditions:

$$w_n(R_o) = 0 \qquad (n = 0...N) \tag{23}$$

$$\frac{1}{3} \sum (h_k^3 - h_{k-1}^3) \left[-d_{110}^{(k)} w_{n,rr} - (n^2 w_n/r^2 + \right.$$

$$\left. + w_{n,r}/r) d_{120}^{(k)} \right] = 0$$

$$\frac{1}{3} \sum (h_k^3 - h_{k-1}^3) \left[-\frac{1}{2} d_{111}^{(k)} w_{n,rr} + (w_{n,r}/r + \right.$$

$$\left. - n^2/r^2) n d_{141}^{(k)} \right]$$

$$\frac{1}{3} \sum (h_k^3 - h_{k-1}^3) \left[-\frac{1}{2} d_{111}^{(k)} w_{n,rr} + d_{141}^{(k)} (w_{n,r}/r - \right.$$

$$\left. w_n/r^2) n \right] = 0$$

$$\frac{1}{3} \sum (h_k^3 - h_{k-1}^3) \left[-\frac{1}{2} d_{112}^{(k)} w_{n,rr} + d_{140}^{(k)} (w_{n,r}/r - \right.$$

$$\left. w_n/r^2) n \right] = 0$$

$$\frac{1}{3} \sum (h_k^3 - h_{k-1}^3) \left[-\frac{1}{2} d_{112}^{(k)} w_{n,rr} + \frac{1}{2} d_{140}^{(k)} (w_{n,r}/r + \right.$$

$$\left. w_{n,r}/r) d_{121}^{(k)} - (w_{n,r} - w_n/r^2) n d_{143}^{(k)} \right] = 0$$

$$\frac{1}{3} \sum (h_k^3 - h_{k-1}^3) \left[\frac{1}{2} (-d_{113}^{(k)} w_{n,rr} - (-n^2 w_n/r^2 + \right.$$

$$\left. + w_{n,r}/r) d_{121}^{(k)} + (w_{n,r}/r - w_n/r^2) n d_{143}^{(k)} \right] = 0$$

$$\frac{1}{3} \sum (h_k^3 - h_{k-1}^3) \left[\frac{1}{2} (-d_{114}^{(k)} w_{n,rr} - (-n^2 w_n/r^2 + \right.$$

$$\left. w_{n,r}/r) d_{122}^{(k)} \right) + d_{142}^{(k)} (w_{n,r}/r - w_n/r^2) n \right] = 0$$

$$\frac{1}{3} \sum (h_k^3 - h_{k-1}^3) \left[-\frac{1}{2} (-d_{114}^{(k)} w_{n,rr} + (-n^2 w_n/r + \right.$$

$$\left. w_{n,r}/r) d_{122}^{(k)} \right) + d_{142}^{(k)} (w_{n,r}/r - w_n/r^2) n \right] = 0 \tag{24}$$

where: $d_{110}^{(k)} = \frac{3}{8} Q_{11}^{(k)} + \frac{2}{8} (Q_{12}^{(k)} + 2Q_{44}^{(k)} + \frac{3}{8} Q_{22}^{(k)})$

$$d_{111}^{(k)} = (Q_{11}^{(k)} - Q_{22}^{(k)}) \frac{4}{8} \cos 2\theta_k$$

$$d_{112}^{(k)} = (Q_{11}^{(k)} - Q_{22}^{(k)}) \frac{4}{8} \sin 2\theta_k$$

$$d_{113}^{(k)} = (Q_{11}^{(k)} \frac{1}{8} - \frac{2}{8} (Q_{12}^{(k)} + 2Q_{44}^{(k)}) + Q_{22}^{(k)} \frac{1}{8}) \cos 4\theta_k$$

$$d_{114}^{(k)} = (Q_{11}^{(k)} \frac{1}{8} - \frac{2}{8} (Q_{12}^{(k)} + 2Q_{44}^{(k)}) + Q_{22}^{(k)} \frac{1}{8}) \sin 4\theta_k$$

$$d_{120} = \frac{1}{8} (Q_{11}^{(k)} + Q_{12}^{(k)} - 4 Q_{44}^{(k)}) + \frac{6}{8} Q_{12}^{(k)}$$

$$d_{121} = [-\frac{1}{8} (Q_{11}^{(k)} + Q_{22}^{(k)} - 4Q_{44}^{(k)}) + Q_{12}^{(k)} \frac{2}{8}] \cos 4\theta_k \tag{25}$$

$$d_{122} = [-\frac{1}{8} (Q_{11}^{(k)} + Q_{22}^{(k)}) - 4Q_{44}^{(k)}) + Q_{12}^{(k)} \frac{2}{8}] \sin 4\theta_k$$

$$d_{140}^{(k)} = \frac{1}{4} (Q_{11}^{(k)} - Q_{22}^{(k)}) \sin 2\theta_k$$

$$d_{141}^{(k)} = \frac{1}{4} (Q_{11}^{(k)} - Q_{22}^{(k)}) \cos 2\theta_k$$

$$d_{142}^{(k)} = \frac{1}{8} (Q_{11}^{(k)} + Q_{22}^{(k)} - 2Q_{12}^{(k)} - 4Q_{44}^{(k)}) \sin 4\theta_k$$

$$c_{1(k)} = \frac{1}{8}(Q_{11}^{(k)} + Q_{22}^{(k)} - 2Q_{12}^{(k)} - 4Q_{44}^{(k)}) \cos 4\theta_k ;$$

$$\theta_k = \alpha_k - \alpha_0$$

The assumed expression for $w_n(r)$ must have at least ten constants and can be described by

$$w_n(r) = (A_{0_n} + a_{1_n} r + a_{2_n} r^2 + a_{3_n} r^3 + a_{4_n} r^4 + a_{5_n} r^5 + a_{7_n} r^7 + a_{8_n} r^8 + a_{9_n} r^9)\, r^{s_n}$$

$$\text{for } n = 0 \ldots N \qquad (26)$$

where s_n is determined from the condition that the determinant of the coefficients must vanish and a_0 to a_3 are considered to be the elements of an eigenvector. Use of the Galerkin procedure leads to the vanishing of n Galerkin integrals, or:

$$\int_0^{R_o} \int_0^{2\pi} [L w_a(r,\theta)]\, w_m(r,\theta)\, r\, dr d\theta = 0;$$

$$\text{for } m = 1,2 \ldots N \qquad (27)$$

Note that use of the Galerkin procedure with an assumed solution which satisfies all the boundary conditions is advantageous only in the case where all boundary conditions are kinematic. In case of natural boundary conditions, the assumed functions must be much more complicated and the procedure might be very tedious.

An alternate approach is offered, which is based on the modified Galerkin procedure as appears in [13]. In this case, the assumed solution must satisfy only the kinematic boundary conditions, and the unknowns are determined through the following modified Galerkin integrals:

$$\int_A [L w_a(r,\theta)]\, w_m(r,\theta)\, dA + \sum_i (M_{rr_a} - \bar{M}_{rr})\Big|_{r=R_i} \times$$

$$w_{m,r}(r = R_i,\theta) + \sum_i (Q_{rr_a} - \bar{Q}_{rr}) \;\Big|\; w_m(r = R_i,\theta) = 0 \;\Big|\; r = R_i$$

$$m = 1,2 \ldots N \qquad (28)$$

where:

M_{rr_a}, Q_{rr_a} are the radial bending moment and shear force determined with the approximate solutions;

$\bar{M}_{rr}$, $\bar{Q}_{rr}$ are the radial bending moment and shear forces applied at the boundaries denoted by the i.

Numerical Results

A computer code has been developed for generating numerical results. The code employs double precision for both the primary state analysis, as well as for the buckling analysis. Results are generated for several symmetric, cantilever geometries, which are quasi isotropic in extension. The plate is made of 2m plies, with fiber orientations $(0^o/\pm 180^o/m)_s$, where m is the number of plies. Note that when m = 3 (three plies), the configuration is $(0^o/60^o/-60^o)_s$; when m = 4, the configuration is $(0^o/45^o/-45^o/45^o)$; and when m = 6, it finally becomes $(0^o/30^o/-30^o/30^o/-30^o/30^o)_s$. All plies are made of the same material, Graphlite/Epoxy (T300-5208), with 70% fiber volume and the following properties

$$E_{11} = 26.3 \times 10^6 \text{ psi} \quad ; \quad E_{22} = 1.49 \times 10^6 \text{ psi}$$

$$\nu_{12} = 0.28 \quad ; \quad \text{and} \quad G_{12} = 1.04 \times 10^6 \text{ psi}$$

The buckling load is nondimensionalized by the quantity $E_{11}h^3/12\, R_o^2(1 - \nu_{12}\nu_{21})$, which is common for all configurations. Thus,

$$\bar{N}_{rr_{cr}} = k_{cr} E_{11} h^3 / 12\, R_o^2\, (1 - \nu_{12}\nu_{21}) \qquad (29)$$

Note that h and R_o are the plate thickness and radius, respectively.

The primary state is solved for by using the procedure, outlined previously, and the functions appearing in Eqs. (13) and (14). The Galerkin integrals are evaluated by using numerical integration with Romberg's extrapolation method. The allowable error is smaller than 10^{-6}.

The approximating series involves functions which are the buckling modes of the corresponding isotropic problem.

$$w_a(r,\theta) = \sum_{n=0}^{N} (J_n(\alpha_n r) + C_{2n} r^n) \cos n\theta$$

where, $J_n(\,)$ are Bessel functions of the first kind of order n; α_n is the square root of the buckling coefficient of the isotropic critical stress resultant (corresponding to the nth mode; if n = 0 α_n = 14.68); and C_{2n} are undetermined constants, evaluated by satisfaction of the boundary conditions.

The limited results are shown graphically on Figs. 2 and 3. Fig. 2 shows a plot of k_{cr} versus m, which implies various quasi-isotropic (in extension) constructions. It is seen from this figure, that k_{cr} is independent of m. This is so because the average flexural stiffnesses, primarily D_{11} & D_{22}, are the same for all m. Next, the configuration corresponding to m = 3 was taken and E_{22}/E_{11} was arbitrarily changed from the correct value of 0.05665 to the value of one (almost isotropic) by keeping the other values constant. It is seen from Fig. 3 that the value of k_{cr} varies from 6.16 to 12.31. Note that the value of k_{cr} for the isotropic construction is 14.68. The difference between the two values is attributed to the effect of the shear stiffness. On Fig. 3, and for $E_{22}/E_{11} = 1$, two additional values of k_{cr} are shown, in order to depict the G-effect.

Acknowledgement

This work was supported by the United States Air Force Office of Scientific Research, under Grant Number AFOSR 83-0243. This financial support is gratefully acknowledged.

REFERENCES

1. Vijayakumar, K., Joga, Rao, C. V., "Buckling of Polar Orthotropic Plates", Journal of EM Div., ASCE, Vol. 97,. EM3, 1971, pp. 701-710.
2. Ramaiah, G. K., Vijayakumar, K., "Buckling of Polar Orthotropic Annular Plates Under Uniform Internal Pressure", AIAA J., Vol. 12, No. 8, 1975, pp. 1048-1050.
3. Uthegenannt E. S., Brand, B. S., "Buckling of Orthotropic Annular Plates", AIAA J., Vol. 8, No 11, 1970, pp. 2102-2104.
4. Harik, I. E., "Analytical Solution to Orthotropic Sectors", Journal of the EM Div., ASCE., Vol. 110, EM4, April 1984, pp. 554-568.
5. Wolnowsky-Krieger, S.,"Uber die Beulsicherheit von Kreisplatten mit kreiszylindrischer Aelotropie", Ingenieur-Archiv, Vol. 26, No. 2, 1958, pp. 129-131.
6. Nowinski, J. L., "Nonlinear Vibration of Elastic Circular Plates Exhibiting Rectilinear Orthotropy", Z. Angew. Math. Phys., Vol. 14, Redaction ZAMP (Germany), 1963, pp. 112-124.
7. Bianchi, A., Aralos, D. R., Laura, P.A.A., "A Note on Transverse Vibrations of Annular Circular Plates of Rectangular Orthotropy", Journal of Sound and Vibrations, Vol. 99, No. 1, 1985, pp. 140-143.
8. Jones, R. M., "Mechanics of Composite Materials," McGraw-Hill Book Company, 1975.
9. Wang, J.T.S., Biggers, S. B., Dickson, J. N., "Buckling of Composite Plates with a Free Edge in Edgewise Bending and Compresson", AIAA Journal, Vol. 22, No. 3, March 1984, pp. 394-398.
10. Leissa, A. W., "Buckling of Laminated Composite Plates and Shell Panels", June 1985, AFWAL-TR-85-3069.
11. Chia, C. Y., "Nonlinear Analysis of Plates", McGraw-Hill International Book Company, 1980.
12. Lekhnitskii, S. G., "Theory of Anistropic Plates", (Translation from Russian), Gordon and Breach Science Publishers, N.Y., 1984.
13. Timtoes, G. J., Elastic Stability of Structures, Prentice-Hall, Inc., Englewood Cliffs, N. J., 1976.

Appendix A: Compliance Matrix Coefficients in θ Coordinates

This appendix outlines the procedure for determining the coefficients of the matrix in terms of the fiber orientation angle of each laminate relative to the θ = 0 axis.

The stress-strain relation for each lamina under consideration is:

$$\begin{Bmatrix} \sigma_1 \\ \sigma_2 \\ \sigma_{12} \end{Bmatrix} = \begin{bmatrix} Q_{11} & Q_{12} & 0 \\ Q_{12} & Q_{22} & 0 \\ 0 & 0 & Q_{44} \end{bmatrix} \begin{Bmatrix} \epsilon_1 \\ \epsilon_2 \\ \gamma_{12} \end{Bmatrix} \qquad (A.1)$$

where: $Q_{11} = \dfrac{E_1}{1-\nu_{12}\nu_{21}}$; $Q_{22} = \dfrac{E_2}{1-\nu_{12}\nu_{21}}$

$$Q_{12} = \frac{\nu_{12}E_2}{1-\nu_{12}\nu_{21}} \qquad Q_{44} = G_{12}$$

Rotation of the compliance matrix, with respect to an angle $(\alpha-\theta)$, yields the following coefficients: where:

$$\bar{Q}_{11} = Q_{11}c^4 + 2(Q_{12} + 2Q_{44})s^2c^2 + Q_{22}s^4$$

$$\bar{Q}_{12} = (Q_{11} + Q_{22} - 4Q_{44})s^2c^2 + Q_{12}(s^4 + c^4)$$

$$\bar{Q}_{22} = Q_{11}s^4 + 2(Q_{12} + 2Q_{44})s^2c^2 + Q_{22}c^4 \qquad (A.2)$$

$$\bar{Q}_{14} = (Q_{11} - Q_{12} - 2Q_{44})sc^3 + (Q_{12} - Q_{22} + 2Q_{44})s^3c$$

$$\bar{Q}_{24} = (Q_{11} - Q_{12} - 2Q_{44})s^3c + (Q_{12} - Q_{22} + 2Q_{44})sc^3$$

$$\bar{Q}_{44} = (Q_{11} + Q_{22} - 2Q_{12} - 2Q_{44})s^2c^2 + Q_{44}(s^4 + c^4)$$

where $c = \cos(\alpha_k - \theta)$ and $s = \sin(\alpha_k - \theta)$

Thus, in the r,θ-coordinate system the stress state is related to the state of strain by:

$$\begin{Bmatrix} \sigma_{rr} \\ \sigma_{\theta\theta} \\ \sigma_{r\theta} \end{Bmatrix} = \begin{bmatrix} \bar{Q}_{11} & \bar{Q}_{12} & \bar{Q}_{14} \\ \bar{Q}_{12} & \bar{Q}_{22} & \bar{Q}_{24} \\ \bar{Q}_{14} & \bar{Q}_{24} & \bar{Q}_{44} \end{bmatrix} \begin{Bmatrix} \epsilon_{rr} \\ \epsilon_{\theta\theta} \\ \gamma_{r\theta} \end{Bmatrix} \qquad (A.2.1)$$

Appendix B: Derivation of the Governing Equations

This appendix is devoted to a detailed derivation of the governing equations. The positive directions of the applied and internal forces are described in Fig. B.1.

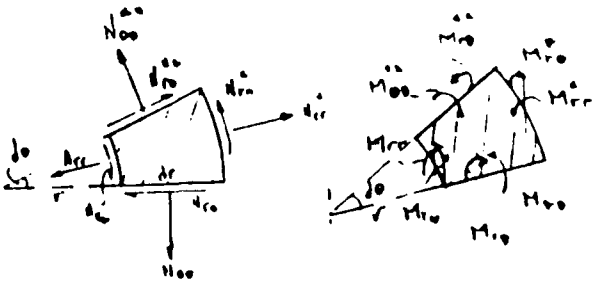

(a) In-plane Resultants Forces (b) Internal Bending and Torsion Moments

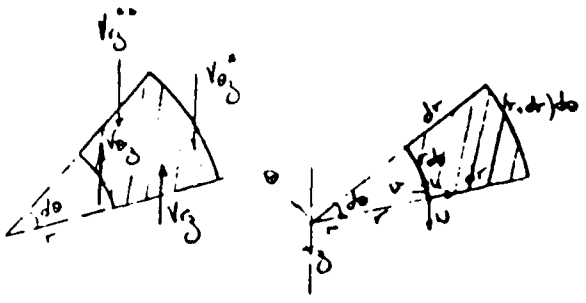

(c) Internal Vertical Shear Forces (d) Positive Deformation

Fig. B.1 Internal Forces & Deformation of Differential Area of the Plate

$( )^{*} = ( ) + ( )_{,r} dr ; ( )^{**} = ( ) + ( )_{,\theta} d\theta$

The in-plane equilibrium equations in terms of the internal forces are:

$$(r N_{rr})_{,r} + N_{r\theta,\theta} - N_{\theta\theta} = 0$$

$$N_{\theta\theta,\theta} + (r N_{r\theta})_{,r} + N_{r\theta} = 0 \qquad (B.1)$$

and the transverse are in terms of inplane forces and internal moments, using the equations above, is

$$(rM_{rr})_{,rr} + 2(M_{r\theta,r\theta} + \frac{1}{r} M_{r\theta,\theta}) +$$

$$(\frac{1}{r} M_{\theta\theta,\theta\theta} - M_{\theta\theta,r}) +$$

$$+ r [N_{rr} w_{,rr} + N_{\theta\theta} (\frac{w_{,\theta\theta}}{r^2} + \frac{w_{,r}}{r}) +$$

$$2N_{r\theta} (\frac{w_{,r\theta}}{r} - \frac{1}{r^2} w_{,\theta})] = 0 \qquad (B.2)$$

The stability governing equations are derived as follows:

$$N_{rr} = N^{o}_{rr} + N^{*}_{rr} \quad ; \quad M_{rr} = M^{*}_{rr} \quad ; \quad w = w^{*} + 0$$

$$N_{\theta\theta} = N^{o}_{\theta\theta} + N^{*}_{\theta\theta} \quad ; \quad M_{\theta\theta} = M^{*}_{\theta\theta} + 0$$

$$N_{r\theta} = N^{o}_{r\theta} + N^{*}_{r\theta} \quad ; \quad M_{r\theta} = M^{*}_{r\theta} + 0 \qquad (B.3)$$

The bending moment and the vertical deflection in the primary state designated with $( )^{o}$ are zero. The additional stress, N^{*}_{ij}, is chosen to be very small compared to N^{o}_{ij}; thus, after substituting it in Eqs. (B.1) and (B.2) yields:

$$(r N^{*}_{rr})_{,r} + N^{*}_{r\theta,\theta} - N^{*}_{\theta\theta} = 0$$

$$N^{*}_{\theta\theta,\theta} + (r N^{*}_{r\theta})_{,r} + N^{*}_{r\theta} = 0 \qquad (B.4)$$

and the buckling equation in the vertical direction is:

$$(r M^{*}_{rr})_{,rr} + 2 (M^{*}_{r\theta,r\theta} + \frac{1}{r} M^{*}_{r\theta,\theta}) +$$

$$(\frac{1}{r} M^{*}_{\theta\theta,\theta\theta} - M^{*}_{\theta\theta,r}) +$$

$$+ [(N^{o}_{rr} + N^{*}_{rr}) w^{*}_{,rr} + (N^{o}_{\theta\theta} + N^{*}_{\theta\theta}) (\frac{w^{*}_{,\theta\theta}}{r^2} + \frac{w^{*}_{,r}}{r})$$

$$+ 2 (N^{o}_{rr} + N^{*}_{r\theta}) (\frac{w^{*}_{,r\theta}}{r} - \frac{1}{r^2} w^{*}_{,\theta})] = 0$$

Since $N^{*}_{ij} << N^{o}_{ij}$, neglect of these terms and omitting the * sign of the deflection and the moments yields:

$$(rM_{rr})_{,rr} + 2 (M_{r\theta,r\theta} + \frac{1}{r} M_{r\theta,\theta}) + (\frac{1}{r} M_{\theta\theta,\theta\theta} -$$

$$M_{\theta\theta,r}) + r [N^{o}_{rr} w_{,rr} + N^{o}_{\theta\theta} (\frac{w_{,\theta\theta}}{r^2} + \frac{w_{,r}}{r}) +$$

$$2 N^{o}_{r\theta} (\frac{w_{,r\theta}}{r} - \frac{1}{r^2} w_{,\theta})] = 0 \qquad (B.5)$$

The kinematic relations used are:
The inplane strain:

$$\varepsilon^{o}_{rr} = u_{,r}$$

$$\varepsilon^{o}_{\theta\theta} = v_{,\theta}/r + u/r \qquad (B.6)$$

$$\gamma^{o}_{r\theta} = 2 \varepsilon^{o}_{r\theta} = v_{,r} + u_{,\theta}/r - v/r$$

The curvatures are:

$$\chi_{rr} = -w_{,rr}$$

$$\chi_{r\theta} = -w_{,\theta\theta}/r^2 - w_{,r}/r \qquad (B.7)$$

$$\chi_{r\theta} = 2\,(-w_{,r\theta}/r + w_{,\theta}/r^2)$$

Using the common assumption in plate theory yields the following relation between the internal forces and the strains and curvatures:

$$\begin{Bmatrix} N^o_{rr} \\ N^o_{\theta\theta} \\ N^o_{r\theta} \end{Bmatrix} = \begin{bmatrix} A_{11} & A_{12} & A_{14} \\ A_{12} & A_{22} & A_{24} \\ A_{14} & A_{22} & A_{44} \end{bmatrix} \begin{Bmatrix} \epsilon^o_{rr} \\ \epsilon^o_{\theta\theta} \\ \gamma^o_{r\theta} \end{Bmatrix} \qquad (B.8)$$

and

$$\begin{Bmatrix} M_{rr} \\ M_{\theta\theta} \\ M_{rr} \end{Bmatrix} = \begin{bmatrix} D_{11} & D_{12} & D_{14} \\ D_{12} & D_{22} & D_{24} \\ D_{14} & D_{24} & D_{44} \end{bmatrix} \begin{Bmatrix} \chi_{rr} \\ \chi_{\theta\theta} \\ \chi_{r\theta} \end{Bmatrix} ; \qquad (B.9)$$

where $A_{ij} = \sum_k \int_{h_{k-1}}^{h_k} \bar{Q}_{ij}\, dz$

$$D_{ij} = \sum_k \int_{h_{k-1}}^{h_k} \bar{Q}_{ij}\, z^2 dz$$

The formulation using deformations u,v and w yields the following governing equations:

$$[r\,(A_{11}u_{,r} + A_{12}v_{,\theta} + A_{14}(u_{,\theta} + v_{,r}))]_{,r} +$$

$$- [(A_{12}u_{,r} + A_{22}v_{,\theta} + A_{24}(u_{,\theta} + v_{,r})]_{,\theta}$$

$$+ [A_{14}u_{,r} + A_{24}v_{,\theta} + A_{44}(u_{,\theta} + v_{,r})]_{,\theta} = 0 \qquad (B.10)$$

$$[A_{12}u_{,r} + A_{22}v_{,\theta} + A_{24}(u_{,\theta} + v_{,r})]_{,\theta} +$$

$$+ [r\,[A_{14}u_{,r} + A_{24}v_{,\theta} + A_{44}(u_{,\theta} + v_{,r})]]_{,r}$$

$$+ A_{14}u_{,r} + A_{24}v_{,\theta} + A_{44}(u_{,\theta} + v_{,r}) = 0 \qquad (B.11)$$

$$[r\,(D_{11}\chi_{rr} + D_{12}\chi_{\theta\theta} + D_{14}\chi_{r\theta})]_{,rr} +$$

$$+ 2\,(D_{14}\chi_{rr} + D_{24}\chi_{\theta\theta} + D_{44}\chi_{r\theta})_{,r\theta}$$

$$+ \frac{2}{r}(D_{14}\chi_{rr} + D_{24}\chi_{\theta\theta} + D_{44}\chi_{r\theta})_{,\theta} +$$

$$+ \frac{1}{r}(D_{12}\chi_{rr} + D_{22}\chi_{\theta\theta} + D_{24}\chi_{r\theta})_{,\theta\theta}$$

$$- (D_{12}\chi_{rr} + D_{22}\chi_{\theta\theta} + D_{24}\chi_{r\theta})_{,r} +$$

$$+ r\,[-N^o_{rr}\chi_{rr} - N^o_{\theta\theta}\chi^o_{\theta\theta} - 2\,N^o_{r\theta}\chi_{r\theta}] = 0 \qquad (B.12)$$

Since the various stiffnesses are θ-dependent, the derivative of the coefficients with respect to θ are different from zero and must be included in the equations.

The in-plane stress distribution can be derived using the Airy function, through the compability equation. The Airy function and stress relations are:

$$N_{rr} = F_{,r}/r + (1/r^2)F_{,\theta\theta}$$

$$N_{\theta\theta} = F_{,rr} \qquad (B.13)$$

$$N_{r\theta} = -(F_{,\theta}/r)_{,r}$$

The compatibility equation is:

$$\epsilon_{rr,\theta\theta} - r\,\epsilon_{rr,r} + r\,(r\,\epsilon_{\theta\theta})_{,rr} +$$

$$- (r\,\gamma_{r\theta})_{,r\theta} = 0 \qquad (B.14)$$

Substituton in Eq. (B.14) and use of Eqs. (B.8) and (B.13) yields:

$$a_{22}F_{,rrrr} - 2a_{24}F_{,rrr\theta}/r + (2a_{12} + a_{44})F_{,rr\theta\theta}/r^2$$

$$-2a_{14}F_{,r\theta\theta\theta}/r^3 + a_{11}F_{,\theta\theta\theta\theta}/r^4 + 2a_{22}F_{,rrr}/r +$$

$$- (2a_{12} + a_{44})F_{,r\theta\theta}/r^3 + 2a_{14}F_{,\theta\theta\theta}/r^4 +$$

$$- a_{11}F_{,rr}/r^2 - 2(a_{14} + a_{24})F_{,r\theta}/r^3 + (2a_{11} +$$

$$2a_{12} + a_{44})F_{,\theta\theta}/r^4 + a_{11}F_{,r}/r^3$$

$$+ 2(a_{14} + a_{24})F_{,\theta}/r^4 = L_F F \qquad (B.15)$$

where L_F is the differential operator described in the equation.

The buckling equation is given by:

$$w_{,rrrr}(rD_{11}) + w_{,rrr}(2D_{11} + 2D_{14,\theta}) + w_{,rrr\theta}(4D_{14})$$

$$+ w_{,rr}(2D_{24,\theta} + 2D_{14,\theta} - D_{22} + D_{12,\theta\theta})/r +$$

$$w_{,rr\theta}(4D_{44,\theta} + 2D_{12,\theta})/r +$$

$$w_{,rr\theta\theta}(2D_{12} + 4D_{44})/r + w_{,r}(D_{22} + D_{22,\theta\theta})/r^2 +$$

$$w_{,r\theta}(4D_{14} - 4D_{44,\theta} + 2D_{24,\theta\theta} + 2D_{22,\theta\theta} + 4D_{24})/r^2 +$$

$$w_{,r\theta\theta}(-2D_{12} - 4D_{44} + 6D_{24,\theta})/r^2 +$$

$$w_{,r\theta\theta\theta}(4D_{24})/r^2 + w_{,\theta}(-4D_{14} + 4D_{44,\theta} + 4D_{24} +$$

$$- 2D_{24,\theta\theta})/r^3 + w_{,\theta\theta}(2D_{12} + 2D_{22} - 6D_{24,\theta} + 4D_{44}$$

$$+ D_{22,\theta\theta})/r^3 +$$

$$w_{,\theta\theta\theta}(-4D_{24} + 2D_{22,\theta})/r^3 + w_{,\theta\theta\theta\theta}(D_{22})/r^3 +$$

$$+ [N^2_{rr}w_{,rr} + N^2_{\theta\theta}(w_{,\theta\theta}/r^2 + w_{,r}/r) +$$

$$+ 2N^2_{r\theta}(w_{,r\theta}/r - w_{,\theta}/r^2)] = 0 \qquad (B.16)$$

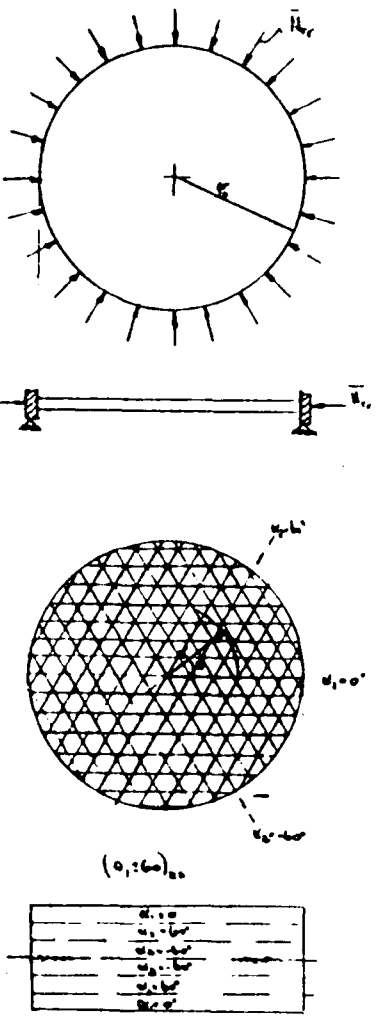

Fig. 1 Load, boundary conditions and geometry of a typical laminated circular plate

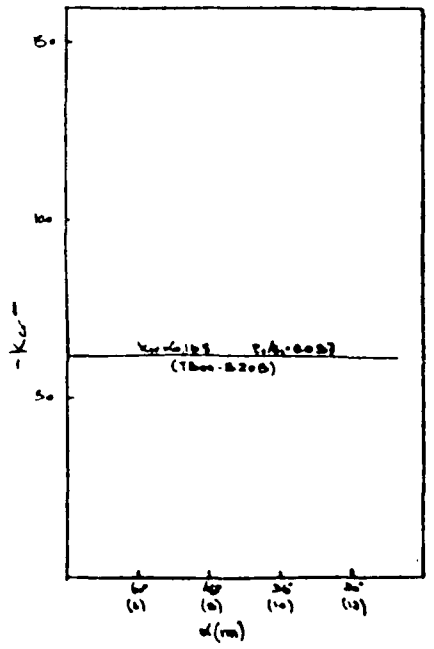

Fig. 2 K_{cr} versus the angle (no. of layer) for a quasi-isotropic (in extension) laminate plate, made of Graphite-Epoxy (T300-5208)

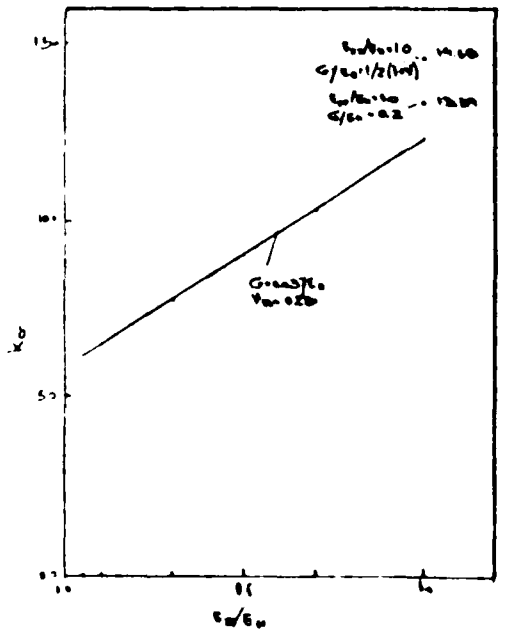

Fig. 3 K_{cr} versus E_{22}/E_{11} for various shear moduli

END

4-87

DTIC